*Nucleic Acids Research*, 2024, **52**, 6906–6927
https://doi.org/10.1093/nar/gkae394
Advance access publication date: 14 May 2024
**Gene regulation, Chromatin and Epigenetics**

# NF-κB factors cooperate with Su(Hw)/E4F1 to balance *Drosophila*/human immune responses via modulating dynamic expression of *miR-210*

**Hongjian Zhou[1,2,†], Yu Huang[1,†], Chaolong Jia[1], Yujia Pang[1,2], Li Liu[1], Yina Xu[1], Ping Jin[1,*], Jinjun Qian[3,*] and Fei Ma[1,*]**

[1]Laboratory for Comparative Genomics and Bioinformatics & Jiangsu Key Laboratory for Biodiversity and Biotechnology, College of Life Science, Nanjing Normal University, Nanjing 210046, China
[2]Institute of Laboratory Medicine, Jinling Hospital, Affiliated Hospital of Medical School, Nanjing University, 210002 Nanjing, Jiangsu, China
[3]School of Medicine & Holistic Integrative Medicine, Nanjing University of Chinese Medicine, 210023 Nanjing, Jiangsu, China.

[*]To whom correspondence should be addressed. Tel: +86 25 85891050; Email: jinping8312@163.com
Correspondence may also be addressed to Jinjun Qian. Email: QianJinjun@njucm.edu.cn
Correspondence may also be addressed to Fei Ma. Tel: +86 25 85891050; Email: mafei01@tsinghua.org.cn
[†]The first two authors should be regarded as Joint First Authors.

## Abstract

MicroRNAs (miRNAs) play crucial regulatory roles in controlling immune responses, but their dynamic expression mechanisms are poorly understood. Here, we firstly confirm that the conserved miRNA *miR-210* negatively regulates innate immune responses of *Drosophila* and human via targeting *Toll* and *TLR6*, respectively. Secondly, our findings demonstrate that the expression of *miR-210* is dynamically regulated by NF-κB factor Dorsal in immune response of *Drosophila* Toll pathway. Thirdly, we find that Dorsal-mediated transcriptional inhibition of *miR-210* is dependent on the transcriptional repressor Su(Hw). Mechanistically, Dorsal interacts with Su(Hw) to modulate cooperatively the dynamic expression of *miR-210* in a time- and dose-dependent manner, thereby controlling the strength of *Drosophila* Toll immune response and maintaining immune homeostasis. Fourthly, we reveal a similar mechanism in human cells, where NF-κB/RelA cooperates with E4F1 to regulate the dynamic expression of *hsa-miR-210* in the TLR immune response. Overall, our study reveals a conservative regulatory mechanism that maintains animal innate immune homeostasis and provides new insights into the dynamic regulation of miRNA expression in immune response.

## Graphical abstract

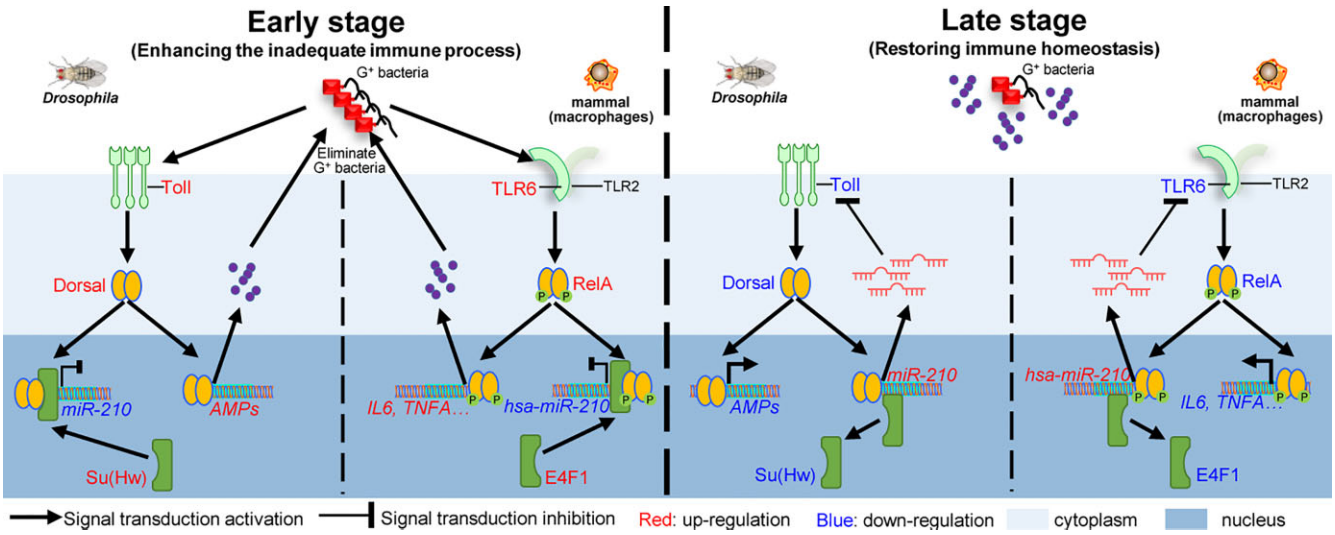


## Introduction

The Toll signaling pathway, initially discovered in *Drosophila melanogaster*, has crucial and evolutionarily conserved functions in innate immune responses across the animal kingdom (1,2). *Drosophila* Toll pathway is mainly responsible for resisting Gram-positive (G+) bacteria or fungi infections

**Received:** January 17, 2024. **Revised:** April 25, 2024. **Editorial Decision:** April 27, 2024. **Accepted:** April 30, 2024

(3). Activation of this pathway induces the nuclear translocation of NF-κB family transcription factors Dorsal and/or Dif (*Dorsal*-related immunity factor) to activate the expression of specific antimicrobial peptide (AMP) genes such as *Drosomycin* (*Drs*) (3,4). However, imbalanced immune responses, either excessive or deficient, can be detrimental to the survival of *Drosophila* (5,6). Therefore, *Drosophila* needs to fine-tune the strength and duration of Toll signaling to maintain immune homeostasis (7). Notably, effective and adequate immune responses of Toll pathway can be intricately regulated by many positive and negative regulators in *Drosophila* (8).

MicroRNAs (miRNAs) as a class of small non-coding RNAs can negatively regulate gene expression to participate in controlling immune responses and maintaining immune homeostasis in animal (9). Currently, some miRNAs, such as *miR-8*, *miR-964*, *miR-958*, *miR-317* and *miR-959-962*, have been demonstrated to negatively regulate *Drosophila* Toll innate immune responses by targeting various genes (10–14). However, how these expressions of immune-specific miRNAs themselves are governed remain unclear. Previous studies have indicated that miRNA expression is usually time-dependent and tissue-specific, which can be controlled by transcription factors (15). For instance, RelA as one human NF-κB factor can directly bind to the promoter regions of certain miRNAs to activate their transcriptions in the biliary epithelial cells (16). However, little is known about whether the *Drosophila* NF-κB factor Dorsal, a core component of Toll pathway controlling the expression of AMPs (17), can also regulate the expression of miRNA during *Drosophila* innate immune responses.

The Suppressor of Hairy-wing [Su(Hw)] is a protein containing 12 zinc finger architectural domains and is known as the best-characterized insulator protein in *Drosophila* (18). In addition to establishing the chromatin insulator of the gypsy retrotransposon (18–21), Su(Hw) may also function as a transcriptional suppressor to repress protein-coding gene transcription in *Drosophila* (22–24). Moreover, studies have shown that most transcription factors lack the effector activity necessary for inducing gene expression, thereby needing to interact with cofactors to regulate cooperatively gene transcription (25,26). For example, NF-κB/RelA can interact with YY1, a member of the Polycomb Group (PcG), to epigenetically suppress *miR-29* expression (27). Interestingly, a recent study using yeast 2-hybrid (Y2H) assays has demonstrated that *Drosophila* NF-κB transcription factors can interact with Su(Hw) protein (28). These above studies led us to speculate that the NF-κB factor Dorsal may interact with transcriptional suppressor Su(Hw) to cooperatively regulate the miRNA expression in *Drosophila* Toll pathway immune responses.

To explore this hypothesis, in the present study, based on the bioinformatic data we firstly predicted the interaction of Su(Hw) and Dorsal with the promoter region of an immune-related *miR-210* from our previous small RNA-seq study (29), and confirmed that *miR-210* was involved in *Drosophila* Toll immune response via directly targeting *Toll in vivo* and *in vitro*. We next demonstrated that infection-induced Dorsal could bind to and repress the promoter activity of *miR-210 in vivo* and *in vitro*, and Dorsal-mediated inhibition required the cooperation with the repressor Su(Hw). Furthermore, the dynamic expression profiles of *Dorsal*, *miR-210*, *Toll*, *Drs* and *su(Hw)* in wild-type flies across 9 time points after *M. luteus* infection provided insights into their critical roles in maintaining strength and persistence of immune response as well as immune homeostasis. Importantly, we also validated that the human NF-κB factor RelA can interact with the zinc-finger protein E4F1 to regulate the dynamic expression of *hsa-miR-210*, thereby controlling the expression level of its target gene *TLR6* to maintaining immune homeostasis in human cell. Overall, our study reveals an evolutionarily conserved mechanism by which NF-κB factors interact with co-repressors to regulate the dynamic expression of *miRNA* for governing innate immune responses and homeostasis in *Drosophila* and human.

## Materials and methods

### Acquisition, construction and maintenance of *Drosophila* strains

Flies were reared on the standard cornmeal/agar/yeast medium at 25°C and 60% humidity. To generate transient overexpressing flies, we performed crosses between UAS-gene transgenic strains and the *Tub-Gal80ts; Tub-Gal4* strain. To minimize lethality during early developmental stages due to the gene requirements in development, all flies were raised in a light-dark (12 h cycle) incubator at a permissive temperature (18°C) until adult progeny of the appropriate genotype emerged. Subsequently, these 4–6 day-old progeny were shifted to restrictive temperature (29°C) for 24 h to induce the overexpression of genes and then infection.

These fly strains, including $w^{1118}$ (BDSC: #3605), *Tub-Gal80*$^{ts}$*; TM2/TM6B* (BDSC: #7019), *Tub-Gal4/TM3, Sb1, Ser1* (BDSC: #5138), UAS-Dorsal (BDSC: #9319), UAS-miR-210 (BDSC: #41179), miR-210 KO (BDSC: #58899), Drs-GFP (BDSC: #55707), *su(Hw) null mutant* (*Df(3R)su(Hw)*$^{7}$*/TM6B, Tb*$^{[1]}$) (BDSC: #1049), *su(Hw) null mutant* ($w^{[1118]}$*; PBac{w[+mC]=RB}su(Hw)*$^{[e04061]}$*/TM6B, Tb*$^{[1]}$) (BDSC:#18224), *Dorsal-GFP* (BDSC:#42677), *su(Hw)-GFP* (BDSC:#64794), *su(Hw)-RNAi* (BDSC:#33906), were obtained from the Bloomington *Drosophila* Stock Center, FlyORF and Tsinghua Fly Center.

To construct the *w*; P{miR-210-EGFP} attP40* fly strain, 1968 bp of DNA immediately upstream of the transcription start site of *miR-210* gene was cloned into Not I/Nde I sites of promoter-EGFP (from Qidong Fungene Biotechnology), which has the attB site and miniwhite marker was used as the backbone. Then 200 embryos were injected using the above plasmid. When the injected P0 embryos grew into adults, they were crossed with Sp/CyO. F1 flies were screened for candidates that carried miniwhite marker in eyes (orange eye). PCR was performed using primers for validation of *miR-210*-EGFP integration. *w*; P{miR-210-Dorsal-motif-mut-EGFP} attP40* and *w*; P{miR-210-su(Hw)-motif-mut-EGFP} attP40* were also constructed by the above method, but the motif sequences of Dorsal and Su(Hw) were mutated during the plasmid construction.

### GFP fluorescence assay and quantification

To verify the AMP activity of *Drs*, *UAS-miR-210* and *miR-210 KO* flies were crossed with the Drs-GFP strain, respectively. To evaluate the promoter activity of *miR-210*-promoter, *miR-210*-promoter-*Dorsal*-motif-mut and *miR-210*-promoter-*su(Hw)*-motif-mut in control and Dorsal overexpression flies *in vivo* post-infection, *UAS-Dorsal* and *Tub-Gal4* flies were crossed with *miR-210-EGFP*, *miR-210-Dorsal-motif-mut-EGFP* and *miR-210-su(Hw)-motif-mut-*

*EGFP* flies, respectively. The GFP fluorescence intensity of 6–10 flies per group was visualized and photographed using fluorescence microscope (Nikon, Japan). ImageJ and GraphPad 8.3 were used for analysis and quantification of the GFP fluorescence intensity.

## Bioinformatics analysis

The mature sequences of *miR-210* and *hsa-miR-210* were downloaded from miRBase (http://www.mirbase.org/). These 3'UTRs of immune-related genes and the promoter sequences of *miR-210* were acquired from the FlyBase (http://flybase.org/) (30). These target genes of *miR-210* were predicted using TargetScan (www.targetscan.org/fly_12/) and miRanda v3.3 with default parameters (31,32). The promoter sequences of *hsa-miR-210* were acquired from NCBI (https://www.ncbi.nlm.nih.gov/) and the target genes of *hsa-mir-210* were predicted from the miRWalk database (http://mirwalk.umm.uni-heidelberg.de/). We predicted these transcription factors that may bind the upstream promoter region of *miR-210* and *hsa-miR-210* based on the PROMO database (http://alggen.lsi.upc.es/cgi-bin/promo_v3/promo/promoinit.cgi?dirDB=TF_8.3/) (33), FIMO (https://meme-suite.org/meme/tools/fimo), Jarspar (http://jaspar.genereg.net/) and TransmiR 2.0 database (http://www.cuilab.cn/transmir). The Venn diagram was drawn on the jvenn website (http://jvenn.toulouse.inra.fr/app/index.html) (34). The regulatory network diagram was drawn by the Cytoscape_v3.7.2. The evolutionary tree was constructed using the IQ-TREE software and visualized using the FigTree v1.4.4. Furthermore, the miRNA promoter sequences were predicted through the BDGP (https://www.fruitfly.org/seq_tools/promoter.html). The human homologous gene is screened using DIOPT v8.0 (http://www.flyrnai.org/diopt). The ChIP-seq of *Drosophila* transcription factors were obtained from ENCODE and modENCODE project (https://www.encodeproject.org/) (35,36). The ChIP-seq peak analysis was conducted by utilizing the ChIPseeker package integrated with R version 4.2.1 (37). Visualization of Dorsal/Su(Hw) ChIP-seq peaks was performed using IGV version 2.9.4 (38).

## Recombinant plasmid construction

The pAc5.1/V5-HisA expression vector (Thermo, USA) was used for constructing the recombinant plasmids. And the luciferase coding sequence was subcloned into pAc5.1/V5-HisA to generate pAc-luc as previous (39). To produce exogenous Dorsal, Su(Hw) in Drosophila S2 cells, the CDS sequences of *Dorsal*, Flag-*su(Hw)* were amplified and cloned into pAc5.1/V5-HisA vector to generate pAc-*Dorsal*-V5, pAc-Flag-*su(Hw)* plasmids using ClonExpress II One Step Cloning Kit (Vazyme, China). The 3' UTR sequences of *Toll* with or without *miR-210* binding sites were amplified by PCR and cloned into pAc-luc to generate pAc-luc-*Toll*-3' UTR and pAc-luc-*Toll*-3' UTR-mut. The promoter region of *miR-210* was predicted by BDGP website (https://www.fruitfly.org/seq_tools/promoter.html). We constructed the promoter region, containing about 2 kb upstream from *miR-210* TSS site, into the pGL3-Basic plasmid (Promega, USA). To exclude the influence of non-specific effects, we constructed the antisense strand sequence of the *hsa-miR-210* promoter into the pGL3-Basic plasmid (pGL3-*hsa-miR-210*-promoter-AS). To explore the cooperative regulation of NF-κB and the zinc finger repressor Su(Hw)/E4F1 on the *miR-210* promoter, we deleted the NF-κB and the zinc finger repressor Su(Hw)/E4F1 motifs in the *miR-210* promoter region using overlap PCR. The 3' UTR sequence of *TLR6* (approximate 4 kb) was extracted from NCBI (https://www.ncbi.nlm.nih.gov/) and the 3' UTR sequence of *TLR6* with or without *hsa-miR-210* binding sites were constructed into psiCHECK-2 plasmid. The CDS sequence of *RelA* and *E4F1* were extracted from NCBI (https://www.ncbi.nlm.nih.gov/) and constructed into CMV-3xFlag and pcDNA3.0-HA plasmids, respectively. All construction ones were verified by Sanger sequencing. All primers used in this analysis were listed in Supplementary Table S2.

## Septic injury and survival experiments

These 4–6 days adult male flies were used for septic injury experiments. The control flies and the flies with over-expressed or knockdown gene/miRNA were infected with *Micrococcus luteus*. Septic injury experiments were performed by pricking the thorax of the flies with a pulled glass capillary carrying M. luteus inoculant using a Nanoject apparatus (Nanoliter 2010, WPI). Next, the flies were collected at specified time-points for subsequent experiments. Survival of infection is the most comprehensive approach to evaluate these immune response deficiencies (40). For survival experiment, the flies were infected with a concentrated culture of *Enterococcus faecalis* as pricking above, and the fly survival rate of 24 h was then recorded in detail.

## Mimics infection and rescue effect verification

For the mimics infection experiment, a pulled glass capillary carrying 2 μM mimics-*miR-210* or negative control mimics-NC (the mimics-NC should be designed based on the sequence of the mimics-miRNA, modifying the mimics-miRNA sequence to contain at least 5-nt mismatches at the 5'-end 'seed site (41)) was injected into the thorax of 4-day-old adult fruit flies. Prior to injection with *M. luteus*, the fruit flies were injected with mimics-NC/mimics-*miR-210* at least 24 h in advance. Samples were then collected at corresponding time points thereafter. To ensure the rescue effect of mimics-*miR-210*, we examined the triglyceride (TG) content and the Nile red-stained lipid droplets in the retinas of 5-day-old $w^{1118}$, *miR-210 KO* and *miR-210* rescued (*miR-210 KO* + *mimics-miR-210*) flies as previously described (42). For TG content analysis, 0.1g of retinas was weighed, and TG was extracted and measured following the instructions of TG Content Assay Kit (Solarbio Life Sciences, #: BC0625, China). To examine lipid droplets in the retinas, the heads of $w^{1118}$, *miR-210 KO* and *miR-210* rescued flies were removed from adult flies and fixed in 4% formaldehyde for 1 h at room temperature. After removing the excess tissues, the retinas were fixed for an additional 30 minutes. Fixed retinas were washed three times (20 min each time) with PBS and then incubated with 1 mg/ml Nile red (Sigma 72485-100MG, 1:1000) for 20 min at room temperature. Subsequently, the retinas were washed three more times (20 min each time). Images were acquired using a Nikon AX confocal microscope.

## RNA extraction and RT-qPCR

First, we collected these treated *Drosophila* adults in five per groups or the treated human cells in 6-well plates at specific time points in DNase/RNase free 1.5 ml EP tubes (Axygen, USA) and quickly frozen in liquid nitrogen. The to-

tal RNA was then extracted in RNA isolators Total RNA Extraction Reagent (Vazyme, China) using a tissue grinder (TIANGEN, China). Total RNA dissolved in DEPC-treated water was tested for concentration and purity with NanoDrop 2000 (Thermo, USA). The samples with *A*260/*A*280 of ∼2.0 and *A*260/*A*230 in the range of 1.8∼2.2 were used to reverse transcription. For RT-PCR, cDNA was prepared by 1 μg RNA each sample using HiScript II Q RT SuperMix for qPCR (Vazyme, China) with 50°C for 15 min and 85°C for 5 s. The stem-loop primers were synthesized for reverse transcription to generate the specific stem-loop cDNA of miRNA. The quantitative PCR reaction was performed on the Roche LightCycler® 96 real-time PCR system (Roche, Switzerland) using AceQ SYBR Green Master Mix (Vazyme, China). The RT-qPCR cycling conditions were: step 1: 95°C for 5 min; step 2: 95°C for 10 s; step 3: 60°C for 30 s, then steps 2 and 3 were cycled for 40 times. Both mRNA and miRNA expression levels were normalized to the control *rp49*/*GAPDH* and *U6* snRNA, respectively. All experiments were performed with three biological replicates and three technical replicates. The relative $2^{-\triangle\triangle CT}$ method was used for data analysis (43). All primers used in this analysis were listed in Supplementary Table S3. All data collected from real-time PCR analysis were presented as means ± SD.

## Cell culture, transfection and immune stimulation

*Drosophila* S2 cells were maintained at 28°C in SFX-insect medium (HyClone, USA) supplemented with 10% fetal bovine serum (FBS), 100 U/ml penicillin and 100 μg/ml streptomycin (Invitrogen, USA). The 293T cells were cultured under standard conditions in Dulbecco's modified Eagle's medium (Wisent, China), 10% fetal bovine serum, 1% penicillin/streptomycin. The THP1 cells were grown in suspension in RPMI/FBS media (RPMI supplemented with 1% of penicillin–streptomycin solution and 15% FBS). The 293T and THP1 cell lines were cultured at 37°C in a 5% $CO_2$ incubator and used within 6 months.

S2 cells, 293T cells and THP1 cells were transiently transfected with the transfection complex in 24-well plates for dual luciferase reporter assay and in 6-well plates for Co-IP or western blot, using X-treme Gene HP Transfection Reagent (Roche, Switzerland). The specific steps of transfection refer to the HP transfection reagent instructions.

THP1 is the monocyte using for studying human innate immunity and can be induced by phorbol-12-myristate-13-acetate (PMA) to become human monocyte-derived macrophages (MDMs) (44), as well as the heat-killed bacteria can induce the innate immune response (45). For immune stimulation, the THP-1 cells were treated with 10 ng/ml of 12-*O*-tetradecanoylphorbol-l3-acetate (PMA) for 36 h. Activated THP-1 cells were differentiated after 36 h in PMA, and then stimulated with PBS or heat-killed *M. luteus* [multiplicity of infection (MOI) = 50] (45).

## Dual luciferase reporter assay

To investigate whether *Toll* is a target gene of *miR-210*, S2 cells were transfected with the mixed transfection complex contained either mimics-*miR-210* or mimics-NC, either pAc-Luc-*Toll*-3′UTR or pAc-Luc-*Toll*-3′UTR-mut and Renilla luciferase plasmid (pRL) for a total volume of 50 μl. Promega pRL was used to normalize the transfection efficiency. To explore whether Dorsal and Su(Hw) could regulate the promoter activity of *miR-210*, we transfected pGL3-*miR-210*-promoter/pGL3-*miR-210*-promoter-*Dorsal*-motif-mut/ pGL3-*miR-210*-promoter-*su(Hw)*-motif-mut, pAc Vector encoding *Dorsal* and *su(Hw)* at different concentrations into S2 cells. For human cells, psiCHECK-2-*TLR6*-3'UTR/ psiCHECK-2-*TLR6*-3'UTR-mut, mimics-*hsa-miR-210*/mimics-NC or pGL3-*hsa-miR-210*-promoter/pGL3-*hsa-miR-210*-promoter-*RelA*-motif-mut/pGL3-*hsa-miR-210*-promoter-*E4F1*-motif-mut, CMV-Flag-*RelA*, pcDNA3.0-HA-*E4F1* were transfected into 293T cells as described above. The luciferase activity was measured using the Dual-Luciferase Reporter Assay System (Promega, USA) according to manufacturer's instructions and the Renilla luciferase activity was used as a control for normalization.

## Chromatin immunoprecipitation (ChIP)

S2 cells transfected with pAc-*Dorsal*-V5 were used for ChIP *in vitro*, while Dorsal-GFP, Su(Hw)-GFP, Su(Hw)-GFP with Dorsal overexpression, Su(Hw)-GFP with Su(Hw) knock down flies and THP1 cells transfected with CMV-Flag-*RelA* and pcDNA3.0-HA-*E4F1* post-infection were prepared for ChIP *in vivo*. The protocol of ChIP is as described in the previous research (39). Briefly, for the ChIP experiment, the cells and ground GFP-tagged flies were fixed at room temperature by crosslinking with a final concentration of 1% formaldehyde solution for 10 min and then quenched with 125 mM glycine for 5 min. After washing twice with cold PBS containing the protease inhibitor cocktail and PMSF, the cells were lysed with cell lysis buffer and nuclear lysis buffer. The clarified lysates were sonicated. The chromatin was then sheared to 200–500 bp. The chromatin was used for ChIP incubating with Dynabeads protein G (Thermo Fisher Scientific, USA) coated with either anti-V5 antibody (ABclonal, #AE017), anti-GFP antibody (abcam, #ab290, USA), anti-Dorsal antibody (DSHB, #7A4-39, USA), anti-RelA Rabbit pAb (ABclonal #A2547, China), anti-E4F1 (D-12) monoclonal antibody (SANTA # sc-514718, USA), rabbit IgG control antibody (ABclonal, #AC005, China) or mouse IgG control antibody (ABclonal, #AC011, China) overnight at 4°C on a rotating platform. After repeated washing with a magnetic rack (Thermo Fisher Scientific, USA), genomic DNA bound to Dorsal/Su(Hw)/RelA/E4F1 was eluted from Dynabeads and then reversed cross-linked overnight at 65°C. The DNA fragments were then purified using AxyPrep PCR Cleanup Kit (Axygen, USA). ChIP-qPCR analysis was performed using DNA from the Input and ChIP experiments using the primers listed in Supplementary Table S4. At least three independent experiments and three technical replicates were performed on the *rp49*, *miR-210* and *Drs* promoters. The *rp49* promoter was used as a negative control and the *Drs* promoter as a positive control.

## Western blot

Protein samples were prepared with RIPA (50 mM Tris–HCl (pH 7.4), 150 mM NaCl, 1% NP-40, 0.1% SDS), and separated by 10% SDS-PAGE gel and then transferred to PVDF membranes. The membranes were blocked with 5% non-fat milk and incubated with the primary antibodies at 4°C overnight. GAPDH primary antibody (36 kDa) (ABclonal #AC001, China), Tubulin β polyclonal antibody (Biogot #AP0064, China), anti-V5 antibody (ABclonal, #AE017, China), anti-Flag antibody (ABclonal, #AE005, China), anti-

HA antibody (ABclonal, #AE008, China), anti-RelA Rabbit mAb (ABclonal #A19653, China), anti-p-RelA (27. Ser 536) Rabbit mAb (ABclonal #AP1294, China), anti-GFP antibody (abcam, #ab290, USA), anti-Dorsal 7A4 (DSHB #AB_528204, USA) and E4F1 (D-12) monoclonal antibody (SANTA # sc-514718, USA) were used at suitable dilution ratio according to the instruction. Then the PVDF membranes were incubated for 1 h∼2 h at room temperature with 1:20,000 horseradish peroxidase (HRP)-conjugated goat anti-rabbit secondary antibody and goat anti-mouse secondary antibody (Biogot #BS13278 #BS12478, China) diluent buffer. The antigen-antibody complex was visualized with an imaging instrument (Li-COR, USA and Clinx, China). The gray value of protein was analyzed using ImageJ.

### Co-immunoprecipitation (Co-IP)

*In vitro* Co-IP experiments were performed using S2 cells transfected and co-transfected with pAc-*Dorsal*-V5 and pAc-Flag-*su(Hw)* plasmids, respectively. For *in vivo* Co-IP experiments, Su(Hw)-GFP flies, with or without infection, were used. Moreover, the 293T cells were transfected and co-transfected with CMV-3xFlag-*RelA* and pcDNA3.0-HA-*E4F1* expression plasmids, respectively, for Co-IP experiments *in vitro* and THP1-induced macrophages, with or without infection, were used for Co-IP experiments *in vivo*. In the Co-IP procedure, 2 $\times$ $10^7$ cells or five flies were collected and suspended in RIPA buffer supplemented with protease inhibitor cocktail (Roche, USA) and PMSF on ice for 30 min. After centrifuging at 13 000 rpm for 10 min at 4°C, the lysates (equal allocation for each IP and Input experiment) were incubated with anti-V5 tag antibody (ABclonal, #AE017, China), anti-Flag tag antibody (ABclonal, #AE005, China), anti-HA tag antibody (ABclonal, #AE008), anti-RelA Rabbit mAb (ABclonal #A19653, China), anti-E4F1 (D-12) monoclonal antibody (SANTA # sc-514718, USA), anti-GFP antibody (abcam, #ab290, USA) and anti-Dorsal 7A4 (DSHB # AB_528204, USA) at 4°C overnight, followed by further incubation with Protein A/G PLUS-Agarose (SANTA,# sc-2003) for 2 h. The beads were washed five times with PBST buffer. The proteins were eluted by Co-IP Elution Buffers (Abmart #T10007, China) and analyzed by western blot with anti-V5 tag antibody (ABclonal, #AE017, China), anti-Flag tag antibody (ABclonal, #AE005, China), anti-HA tag antibody (ABclonal, #AE008), anti-RelA Rabbit mAb (ABclonal #A19653, China), anti-E4F1 (D-12) monoclonal antibody (SANTA # sc-514718, USA), anti-GFP antibody (abcam, #ab290, USA) and anti-Dorsal 7A4 (DSHB # AB_528204, USA).

In *Drosophila*, the *in vitro* Co-IP experiments were conducted using S2 cells that IP with anti-IgG or overexpressed Dorsal-V5 and Flag-Su(Hw), respectively, serving as a control. The total protein amount in the input sample was determined using anti-Tubulin. The output had been shown to evaluate the effectiveness of the IP. While input and all IP groups had been shown on the same gel for evaluation. WB gray scale analysis via ImageJ was used to quantify the percentage of input relative to the IP. For *in vivo* Co-IP experiments, we equally divided the lysates into four aliquots for each IP/Input experiment and also used anti-IgG as a control. The effectiveness of the IP was assessed using the output from these experiments. Similar to the *in vitro* experiments, the input and all IP groups had been shown on the same gel for evaluation. WB gray scale analysis via ImageJ was again used to quantify the percentage of input relative to the IP. The Co-IP assay performed in human cells were consistent with flies.

### RNA-immunoprecipitation (RIP)

The main RIP experimental steps refer to this protocol (46,47). In brief, about 2 $\times$ $10^7$ 293T cells transfected with mimics-NC or mimics-*hsa-miR-210* were lysed in RIPA buffer (Beyotime Biotechnology, China) containing the PMSF (Beyotime Biotechnology, China), protease inhibitor cocktail (Roche, Switzerland) and RNase inhibitor (Thermo Fisher Scientific, USA) for 30 min on ice. The supernatants after high-speed centrifugation were pre-cleared for 2 h using protein A agarose (Invitrogen, Carlsbad, CA, USA) at 4°C and take 10% as 'Input'. After pre-clearing, anti-Ago2 antibody (Thermo, #AB_2576596, USA) were added in the supernatants and incubated at 4°C overnight. The next day, protein A agarose was joined and rotating incubated for 2 h. The agarose beads were washed using RIPA buffer for five times. The IP complexes were eluted using TE buffer with 1% (w/v) SDS. The eluted complexes of Ago2 and RNA were treated with protease K to separate the protein-bound RNA, and RNA was extracted and quantified using RT-qPCR.

### Quantification and statistical analysis

All experimental data in this work were collected from three independent biological replicates. All statistical analyses were presented as means ± SD. Significant differences between the values under different experimental conditions were subjected to two-tailed Student's *t*-test. Statistical analysis of fly survival experiments was performed using the log-rank (Mantel–Cox) test. All graphs were drawn by the Graphpad prism 8.3. For all tests, $P$ value <0.05 was considered as statistically significant. $^*P < 0.05$; $^{**}P < 0.01$; $^{***}P < 0.001$ and ns, no significance versus the control groups.

## Results

### *miR-210* negatively regulates *Drosophila* Toll signaling via directly targeting *Toll*

We firstly used different fly strains to explore the roles of *miR-210* in immune responses. Our results demonstrated that the expression level of the signature antimicrobial peptide *Drosomycin* (*Drs*) mRNA in the *miR-210* overexpression (*miR-210 OE*) flies (*Gal80$^{ts}$/+; Tub-Gal4/UAS-miR-210*) decreased by 20%, 30%, 25% compared to the control ones (*Gal80$^{ts}$/+; Tub-Gal4/+*) at 6 h, 12 h, 24 h after infection with *M. luteus*, respectively, with no significant differences between the transgenic fly strain (*Gal80$^{ts}$/+; UAS-miR-210/+*) and the control Gal4 flies (*Gal80$^{ts}$/+; Tub-Gal4/+*) (Figure 1A and Supplementary Figure S1A). In contrast, the expression level of *Drs* in the *miR-210* knockout (*miR-210 KO*) flies increased by 22%, 50% and 70% at 6, 12 and 24 h after infection compared to the control ones (*w$^{1118}$*), respectively (Figure 1B). Of note, the expression level of *Drs* in the *miR-210* rescued flies (*miR-210 KO* + *mimics-miR-210*) was almost restored to the level in the control flies (*w$^{1118}$*) (Figure 1B and Supplementary Figure S1B–G). Especially, similar results were also observed for other AMPs *Defensin* (*Def*), *Drosocin* (*Dro*) and *Metchnikowin* (*Mtk*) (Supplementary Figures S2A and B). Therefore, *Drs* was chosen as a representative AMP to detect Toll immune response in the following studies. Subsequently, we used the *Drs-GFP* reporter fly strains to examine the

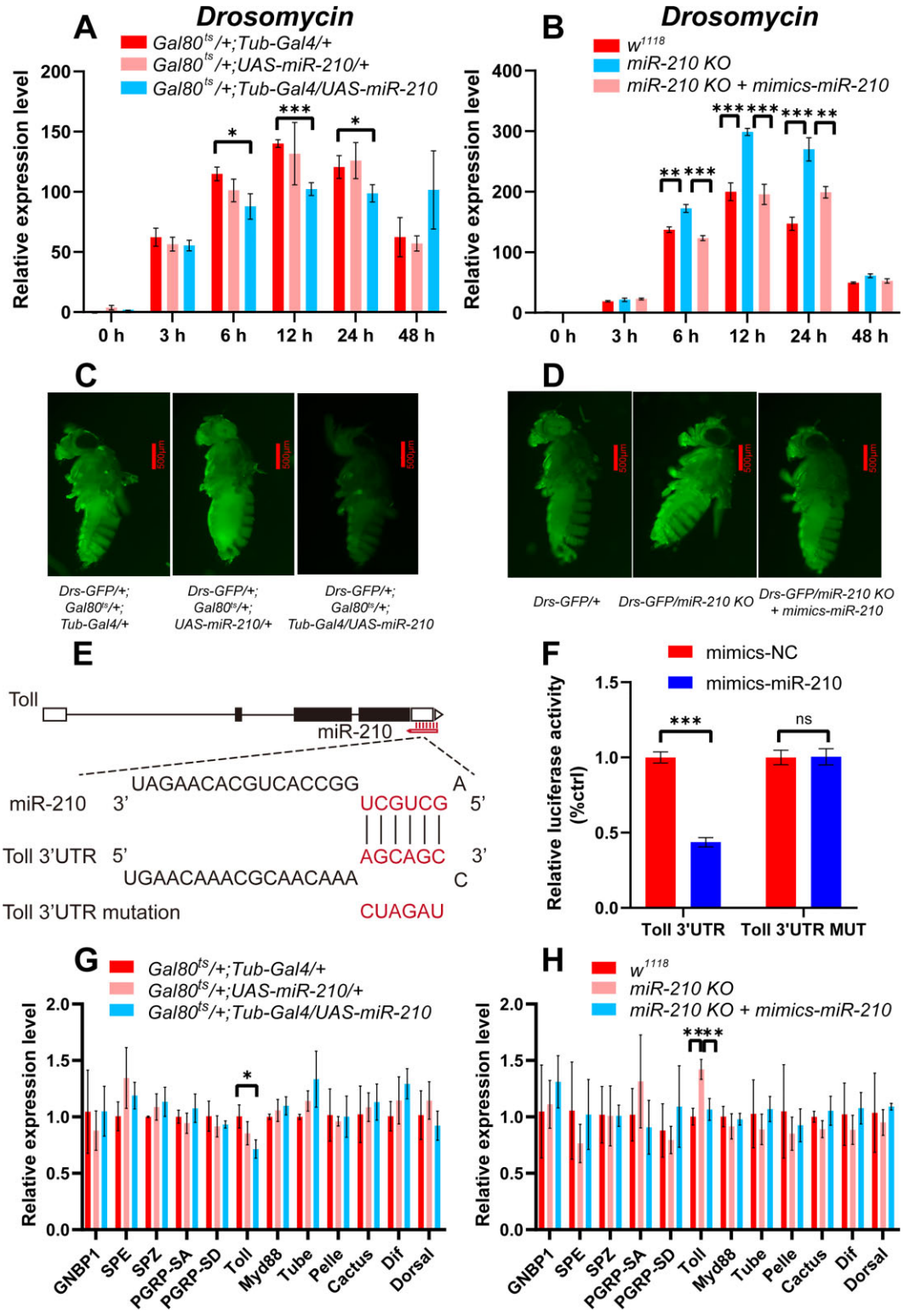


**Figure 1.** *miR-210* negatively regulates *Drosophila* Toll signal via targeting *Toll* (**A**) RT-qPCR analysis of *Drs* `expression in the control flies (*Gal80$^{ts}$/+; Tub-Gal4/+* and *Gal80$^{ts}$/+; UAS-miR-210/+*) and the *miR-210* overexpressed flies (*Gal80$^{ts}$/+; Tub-Gal4/UAS-miR-210*) at different time points after *M. luteus* infection. (**B**) RT-qPCR analysis of *Drs* expression in the control flies (*w$^{1118}$*), the *miR-210 KO* flies and the *miR-210* rescued flies (*miR-210 KO + mimics-miR-210*) at different time points after *M. luteus* infection. (**C**) Fluorescence microscopy images show the fluorescence intensity of Drosomycin-green fluorescent protein (Drs-GFP) in control flies (left and middle) and the *miR-210* overexpressed flies (right) at 12 h after M. luteus infection. (**D**) Fluorescence microscopy images show the fluorescence intensity of Drs-GFP in control flies (left), the *miR-210 KO* flies (middle) and the *miR-210* rescued flies (right) at 12 h after M. luteus infection. (**E**) Predicted binding sites of *miR-210* in 3'UTR region of *Toll* were identified using TargetScan software. The 3'UTR target sequences were mutated base on the *miR-210* seed sequence. (**F**) Dual luciferase assay was performed in *Drosophila* S2 cells to measure the luciferase activities of mimics-*miR-210* and a reporter plasmid with or without a mutation in the target site of *Toll*. (**G**) RT-qPCR analysis of 12 Toll pathway genes in control flies and the *miR-210* overexpressed flies. (**H**) RT-qPCR analysis of 12 Toll pathway genes in control flies, *miR-210 KO* flies, and *miR-210* rescued flies.

expression level of Drs protein, and observed a significantly reduced Drs-GFP intensity in the *miR-210 OE* flies (*Drs-GFP/+; Gal80$^{ts}$/+; Tub-Gal4/UAS-miR-210*) compared to the control flies (*Drs-GFP/+; Gal80$^{ts}$/+; Tub-Gal4/+*), with no significant difference between the two control files (*Drs-GFP/+; Gal80$^{ts}$/+; UAS-miR-210/+* and *Drs-GFP/+; Gal80$^{ts}$/+; Tub-Gal4/+*) (Figure 1C and Supplementary Figure S2C). On the contrary, the Drs-GFP intensity in the *miR-210 KO* flies (*Drs-GFP/miR-210 KO*) was significantly increased compared to the control flies (*Drs-GFP/+*), and the Drs-GFP intensity in the *miR-210* rescued flies (*Drs-GFP/miR-210 KO + mimics-miR-210*) returned to near-normal levels (*Drs-GFP/+*) (Figure 1D and Supplementary Figure S2D). These above results demonstrated an important role of *miR-210* in negatively regulating *Drosophila* Toll immune responses.

We further predicted potential targets of *miR-210* (Supplementary Figure S2E), and found that only target gene *Toll* was the key effector of Toll signaling pathway among 16 potential targets identified (Supplementary Figure S2F). We next used the dual luciferase reporter assays to validate whether *miR-210* can target *Toll* in *Drosophila* S2 cells. Our results showed the luciferase activity of pAc-luc-*Toll*-3'UTR was repressed by 60% using mimics-*miR-210* transfection compared to the negative control (mimics-NC), which was abolished when the binding site was mutated in the 3' UTR of *Toll*, indicating that *miR-210* could bind and repress *Toll* gene *in vitro* (Figure 1E and F). To exclude other potential targets of *miR-210*, we further detected the expression levels of 12 known Toll pathway genes (*GNBP1*, *SPE*, *SPE*, *PGRP-SA*, *PGRP-SD*, *Toll*, *Myc88*, *Tube*, *Pelle, Cactus*, *Dif*, *drosal*) using the aforementioned fly strains, confirming that only the expression level of *Toll* exhibited significant decreases in the *miR-210 OE* flies, increased in the *miR-210 KO*, and restored in the *miR-210* rescued flies (Figure 1G and H). Accordingly, the expression level of four AMPs in the *Toll-RNAi* flies (*Gal80$^{ts}$/+; Tub-Gal4/UAS-Toll-RNAi*) was significantly lower than those in the control flies (*Gal80$^{ts}$/+; Tub-Gal4/+*) (Supplementary Figure S2G). Collectively, our results supported that *miR-210* could negatively regulate Toll pathway only via directly targeting *Toll*.

## Dorsal inhibits *miR-210* transcription via binding to its promoter region

We identified two potential transcription start sites (TSS) at –505 and –177 upstream of the left arm of *miR-210* gene based on the BDGP website, and predicted the binding of the NF-κB transcription factor Dorsal to the promoter region of *miR-210* (Figures 2A, Supplementary Figure S3A, C and E). Meanwhile, the ChIP-seq data analysis revealed a distinct peak of Dorsal on the *miR-210* promoter (Figures 2B). We thus constructed the two promoter fragments, i.e. the pGL3-*miR-210*-TSS1 of 1531 bp and the pGL3-*miR-210*-TSS2 of 1842 bp covering both TSS1 and TSS2, into the pGL3-Basic plasmid, respectively (Figures 2A). Our results demonstrated that the promoter activity of TSS2 was stronger than that of TSS1 (Figures 2C). Remarkably, the promoter activity of *miR-210* was significantly decreased when co-transfecting exogenously expressed Dorsal (pGL3-*miR-210*-TSS-1/2 + pAc-*Dorsal*) compared to the controls (pGL3-*miR-210*-TSS-1/2 + pAc-empty) (Figures 2D). Consistently, the expression level of *miR-210* was significantly decreased to about 60-70% in the *Dorsal* overexpressed flies (*Gal80$^{ts}$/UAS-Dorsal; Tub-Gal4/+*) compared to the control flies (*Gal80$^{ts}$/+; Tub-Gal4/+*) *in vivo* (Figures 2G). The known positive control *Drs*, one AMP gene known to be regulated by Dorsal (48), was used to solidify the accuracy of the above results *in vitro* and *in vivo* (Figures 2A, E, F and H). Additionally, the results of *in vitro* ChIP-qPCR experiments showed that the enrichment signal of Dorsal was 2.2% of Input for the positive control *Drs* promoter region, 1.2% of Input for the *miR-210* promoter, and only 0.15% for the negative control *rp49*, whereas the enrichment signal of the negative control anti-IgG for the promoter region of *rp49*, *Drs* and *miR-210* was all about 0.15% (Figures 2I). Consistently, these results from *in vivo* ChIP-qPCR experiments also demonstrated that the enrichment signal of Dorsal was 0.8% of Input for the positive control *Drs* promoter, 0.7% of Input for the *miR-210* promoter, but only 0.15% for the negative control *rp49* promoter (Figures 2J). Together, these above *in vitro* and *in vivo* results revealed that Dorsal can bind to the promoter region of *miR-210* and inhibit *miR-210* transcription.

## Dorsal inhibits *miR-210* transcription to de-suppress *Toll* expression

The mRNA expression levels of *Drs* and target gene *Toll* were also further tested in the *Dorsal* overexpressed flies (*Gal80$^{ts}$; Tub-Gal4>Dorsal + mimics-NC*), the *Dorsal + miR-210* co-overexpressed flies (*Gal80$^{ts}$; Tub-Gal4>Dorsal + mimics-miR-210*) and the controls (*Gal80$^{ts}$; Tub-Gal4/+ + mimics-NC*) with or without *M. luteus* infection. Our results showed that the expression level of *Drs* in the *Dorsal* overexpressed flies was 80 folds higher than that of the controls under no infection condition, especially the expression level of *Drs* in the *Dorsal + miR-210* co-overexpressed flies was returned to 50% of that in the *Dorsal* overexpressed flies (Figures 3A, Supplementary Figure S4A and B). Similarly, the expression level of *Toll* was increased in the *Dorsal* overexpressed flies and restored to that of the controls in the *Dorsal + miR-210* co-overexpressed flies (Figures 3B). Meanwhile, at the early stage of *Drosophila* immune response to *M. luteus* infection (3 h post-infection), we observed a similar expression profile for both *Toll* and *Drs* but with less altered folds for *Drs* and *Toll* (Figures 3C and D). These results demonstrated that Dorsal can promote *Drosophila* immune response through repressing *miR-210* transcription to de-suppress target gene *Toll* in the early stage of *Drosophila* immune response.

Herein, we further examined whether *miR-210* could affect the survival of the above fly strains upon infected using the lethal G+ bacteria *E. faecalis*. Our results indicated that the survival rate of the *Dorsal* overexpressed flies was significantly higher than that of the controls. Whereas, the survival rate of the *Dorsal + miR-210* co-overexpressed flies was significantly shortened than the *Dorsal* overexpressed flies (Figures 3E). Overall, these above findings revealed that the fine-tune regulation of *miR-210* expression by Dorsal is essential for maintaining *Drosophila* immune homeostasis and survival.

## Su(Hw) is required for Dorsal-mediated transcriptional repression of *miR-210*

Previous studies have indicated the Dorsal-mediated transcriptional repression was dependent on co-factors such as *groucho* and *AP-1* (49,50). Here, we predicted the binding of a known transcriptional suppressor Su(Hw) to the promoter of *miR-210* based on the ENCODE database and the TransmiR

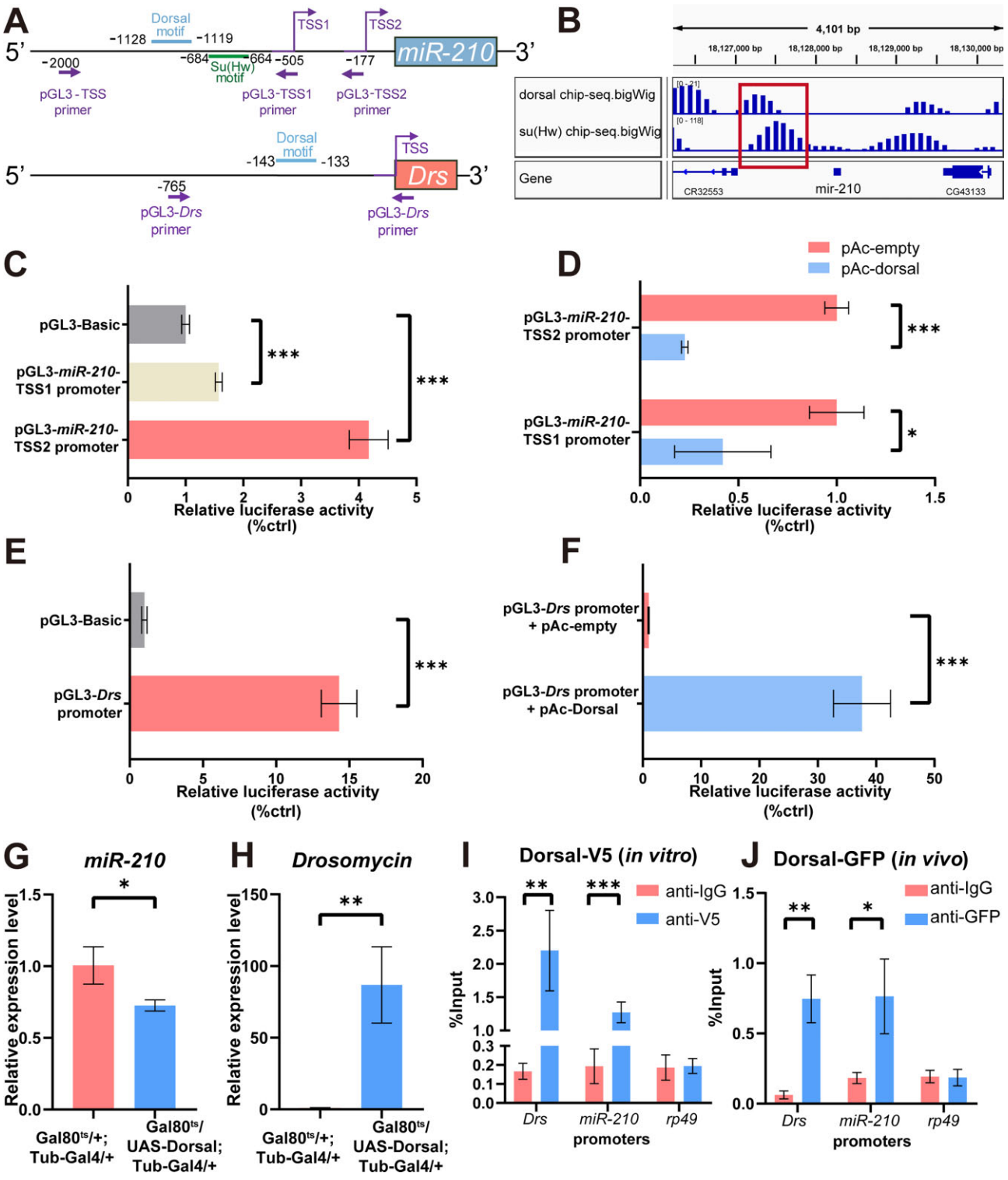


**Figure 2.** Dorsal inhibits *miR-210* transcription via binding to its promoter region (**A**) Schematic diagram depicts the promoter region of *miR-210* and *Drs*. The predicted transcription start sites (TSS) and primer positions were indicated by a purple line. Predicted Dorsal motifs (blue line) and Su(Hw) motifs (green line) were shown at the promoter region of *miR-210*. (**B**) Visualization of ChIP-seq data for Dorsal and Su(Hw) using IGV. The red box indicates the peaks of Dorsal and Su(Hw) at the *miR-210* promoter region. (**C**) Promoter activities of *miR-210*-TSS1 and *miR-210*-TSS2 were determined in *Drosophila* S2 cell using a luciferase assay. (**D**) Promoter activities were determined for *miR-210*-TSS1 and *miR-210*-TSS2 in the presence or absence of exogenous Dorsal in *Drosophila* S2 cell using a luciferase assay. (**E**) Promoter activities of *Drs* were determined in *Drosophila* S2 cell using a luciferase assay. (**F**) Promoter activities were determined for *Drs* in the presence or absence of exogenous Dorsal in *Drosophila* S2 cell using a luciferase assay. Remarkably, Fig. 2C and 2E were normalized against pGL3-Basic, Fig. 2D was normalized to pGL3-*miR-210*-TSS2 promoter + pAc-empty and pGL3-*miR-210*-TSS1 promoter + pAc-empty respectively, and Fig 2F was normalized against pGL3-*Drs* promoter + pAc-empty. (**G**) RT-qPCR analysis of *miR-210* was detected in the *Dorsal* overexpressed flies (*Gal80$^{ts}$/UAS-Dorsal; Tub-Gal4/+*), normalized to the controls (*Gal80$^{ts}$/+; Tub-Gal4/+*). (**H**) RT-qPCR analysis of *Drs* was detected in the *Dorsal* overexpressed flies (*Gal80$^{ts}$/UAS-Dorsal; Tub-Gal4/+*), normalized to the controls (*Gal80$^{ts}$/+; Tub-Gal4/+*). (**I**) ChIP-qPCR was performed to detect the fold change in Dorsal binding on the promoters of *miR-210*, *Drs* and *rp49 in vitro*. (**J**) ChIP-qPCR analysis of Dorsal binding on the promoters of *miR-210*, *Drs* and *rp49 in vivo*.

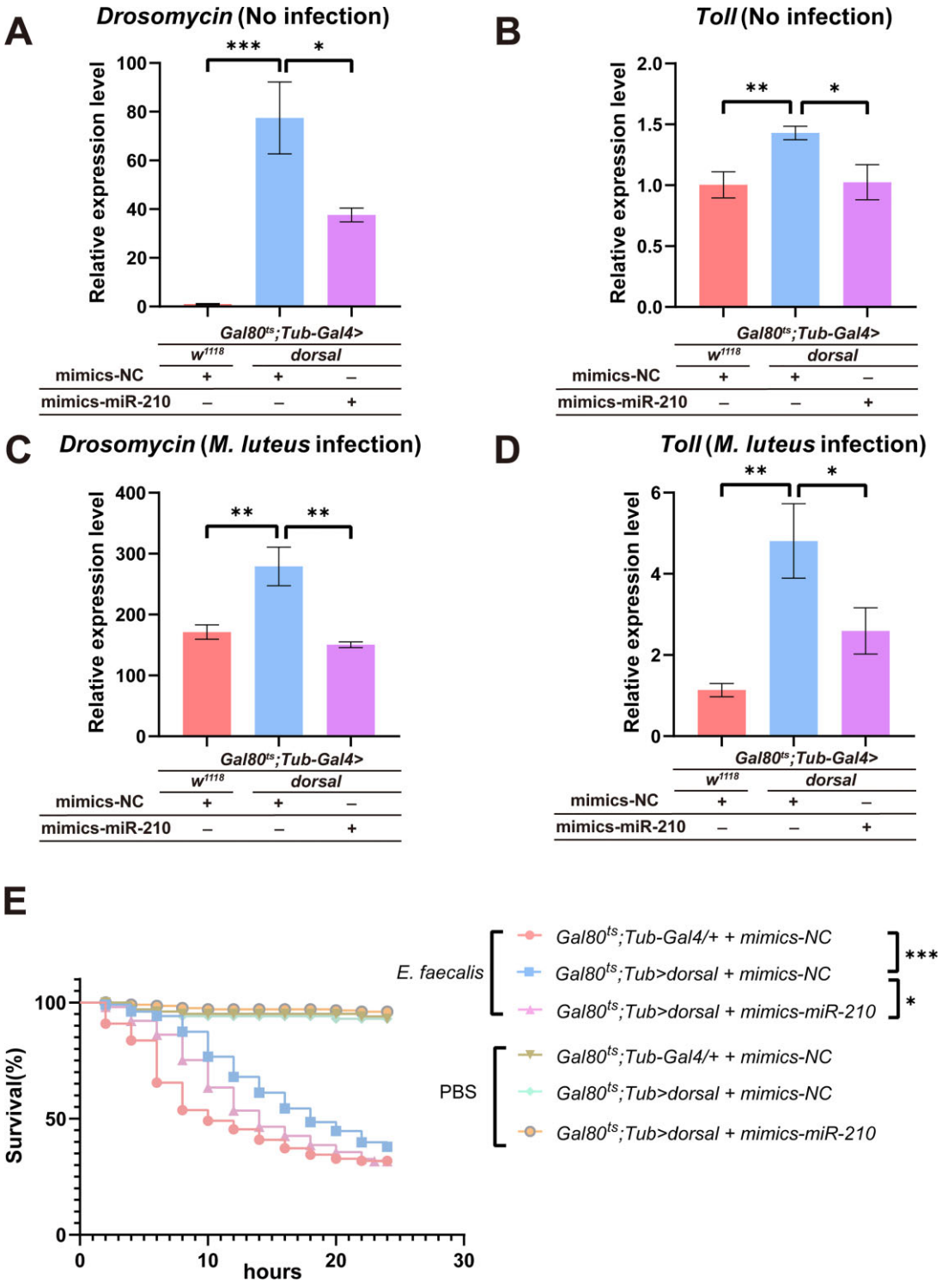


**Figure 3.** Dorsal inhibits *miR-210* transcription to de-suppress *Toll* expression (**A**) The expression levels of *Drs* were examined in the control flies (*Gal80$^{ts}$/+; Tub-Gal4/+ +* mimics-NC), the *Dorsal* overexpressed flies (*Gal80$^{ts}$; Tub> UAS-Dorsal +* mimics-NC), the *Dorsal* and *miR-210* co-overexpressed flies (*Gal80$^{ts}$; Tub> UAS-Dorsal + mimics-miR-210*) before infection. (**B**) The expression levels of *Toll* were examined in the control flies (*Gal80$^{ts}$/+; Tub-Gal4/+ +* mimics-NC), the *Dorsal* overexpressed flies (*Gal80$^{ts}$; Tub> UAS-Dorsal +* mimics-NC), the *Dorsal* and *miR-210* co-overexpressed flies (*Gal80$^{ts}$; Tub> UAS-Dorsal + mimics-miR-210*) before infection. (**C**) The expression levels of *Drs* were examined in the control flies (*Gal80$^{ts}$/+; Tub-Gal4/+ +* mimics-NC), the *Dorsal* overexpressed flies (*Gal80$^{ts}$; Tub> UAS-Dorsal +* mimics-NC), the *Dorsal* and *miR-210* co-overexpressed flies (*Gal80$^{ts}$; Tub> UAS-Dorsal + mimics-miR-210*) at 3 h after *M. luteus* infection. (**D**) The expression levels of *Toll* were examined in the control flies (*Gal80$^{ts}$/+; Tub-Gal4/+ +* mimics-NC), the *Dorsal* overexpressed flies (*Gal80$^{ts}$; Tub> UAS-Dorsal +* mimics-NC), the *Dorsal* and *miR-210* co-overexpressed flies (*Gal80$^{ts}$; Tub> UAS-Dorsal + mimics-miR-210*) at 3 h after *M. luteus* infection. (**E**) Survival rate changes were monitored for 24 h in the *Dorsal* over-expressed flies, the *Dorsal* and *miR-210* co-overexpressed flies and the control flies with PBS as well as *E. faecalis* infection. Survival rates: *Gal80$^{ts}$; Tub-Gal4/+ +* mimics-NC—*E. faecalis* ($n = 110$); *Gal80$^{ts}$; Tub> UAS-Dorsal +* mimics-NC—*E. faecalis* ($n = 103$); *Gal80$^{ts}$; Tub> UAS-Dorsal + mimics-miR-210*—*E. faecalis* ($n = 101$); *Gal80$^{ts}$; Tub-Gal4/+ +* mimics-NC—PBS ($n = 103$); *Gal80$^{ts}$; Tub> UAS-Dorsal +* mimics-NC—PBS ($n = 102$); *Gal80$^{ts}$; Tub> UAS-Dorsal + mimics-miR-210*—PBS ($n = 104$).

v2.0 database (Figures 2A, 4A, Supplementary Figure S3 and Supplementary Table S1) (51,52), implying that Su(Hw) may be involved in Dorsal-mediated transcriptional repression of *miR-210*. Of note, our results demonstrated the increased expression level of *miR-210* by ∼ 50% in two *su(Hw)* null mutation flies (*Df(3R)su(Hw)*$^{7}$ and *PBac{RB}su(Hw)*$^{e04061}$) compared to the control flies (*w*$^{1118}$) *in vivo* post-infection (Supplementary Figure S4C). We next examined the effect of different concentrations of Dorsal and Su(Hw) on *miR-210* promoter activity (pGL3-*miR-210*-TSS2) by transfecting serial dosages of pAc-*Dorsal*-V5/pAc-Flag-*su(Hw)* plasmids (500, 1000 and 1500 ng) into S2 cells. Our dual luciferase reporter results showed that *miR-210* promoter activity could be suppressed by exogenously overexpressed either Dorsal or Su(Hw) in a dose-dependent manner (Supplementary Figure S4E and F). Especially, we found that the co-overexpression of Dorsal and Su(Hw) could result in a stronger inhibition of *miR-210* promoter activity compared to their separate overexpression (Figure 4B). When the *Dorsal* binding motif in the *miR-210* promoter was mutated, the overexpression of Su(Hw) alone or the co-overexpression of Dorsal and Su(Hw) significantly repressed the *miR-210* promoter activity, but their inhibitory effects were similar (Figure 4C). Conversely, once the Su(Hw) binding motif was mutated, the overexpression of Dorsal alone or the co-overexpression of Dorsal and Su(Hw) both significantly enhanced the promoter activity of *miR-210* (Figure 4D). Remarkably, there seemed to be no genetic indirect interaction between Dorsal and Su(Hw) due to no difference in *su(Hw)* mRNA levels between the *Dorsal*-OE flies and the control flies (Supplementary Figure S4G), as well as no significant change in the *Dorsal* expression level between the *su(Hw)* null mutant flies and the controls (Supplementary Figure S4H). These above results suggested that Dorsal-mediated transcriptional repression of *miR-210* might depend on Su(Hw).

We further generated three *Drosophila* strains: *miR-210-promoter-EGFP* (*miR-210-EGFP*), *miR-210-promoter-Dorsal-motif-mut-EGFP* (*miR-210-Dorsal-motif-mut-EGFP*) and *miR-210-promoter-su(Hw)-motif-mut-EGFP* (*miR-210-su(Hw)-motif-mut-EGFP*), which were crossed with the *Dorsal*-OE flies and the control flies. We compared the GFP fluorescence intensity of these strains at 3 h post-infection, and found that Dorsal overexpression considerably suppressed GFP fluorescence intensity in the *miR-210-EGFP* flies compared to the controls (Figure 4E and F), but had no significant effect on the *miR-210-Dorsal-motif-mut-EGFP* flies (Figure 4G and H). In contrast, Dorsal overexpression significantly enhanced GFP intensity in the *miR-210-su(Hw)-motif-mut-EGFP* flies (Figure 4I and J). Taken together, these *in vitro* and *in vivo* results indicated that Su(Hw) is required for Dorsal-mediated suppression of *miR-210* during *Drosophila* Toll immune response.

## Infection-induced Dorsal interacts with Su(Hw) to suppress *miR-210* transcription

The previous study reported a potential direct interaction between Su(Hw) and NF-κB family transcription factors using yeast 2-hybrid assays (28). Interestingly, we also observed the overlapped ChIP-seq peak between Dorsal and Su(Hw) within the promoter region of *miR-210* (Figure 2B). We thus hypothesized that Dorsal and Su(Hw) may cooperate to regulate *miR-210* expression.

To prove this hypothesis, we firstly co-transfected pAc-*Dorsal*-V5 and pAc-*Flag*-su(Hw) plasmids or alone, and then performed the immunoprecipitation (IP) assay using antibodies anti-V5 for Dorsal and anti-Flag for Su(Hw) in S2 cells. Our results showed that after IP with anti-Flag antibodies, western blot could clearly detect Dorsal-V5 and vice versa (Figure 5A, quantified in Supplementary Figure S7A and B). We further conducted an *in vivo* co-IP assay using antibodies against Dorsal and GFP in Su(Hw)-GFP flies, and found that there was no interaction between Dorsal and Su(Hw) under non-infected conditions (Figure 5B), but a clear interaction between Dorsal and Su(Hw) was detected at 3 h post-infection (Figure 5B, quantified in Supplementary Figure S7C and D). Additionally, we examined the signals of Dorsal and Su(Hw) within the *miR-210* promoter region using anti-Dorsal or anti-GFP antibodies at 3 h post-infection in the *Dorsal*-OE (*su(Hw)-GFP/UAS-Dorsal; Tub-Gal4/+*) flies and the *su(Hw)*-RNAi (*+/su(Hw)-GFP; Tub-Gal4/UAS-su(Hw)-RNAi*) flies, respectively. These results demonstrated that Dorsal overexpression significantly increased the signal of Dorsal within the *miR-210* promoter region, especially this increase was accompanied by a significant increase of the Su(Hw) signal within the *miR-210* promoter region, implying that Dorsal could interact with Su(Hw) to bind to the *miR-210* promoter region (Figure 5C and D). To further reveal whether perturbation of Su(Hw) affects Dorsal signals in the *miR-210* promoter, we knocked down Su(Hw) in *Drosophila* and examined the signals of Dorsal and Su(Hw) in the *miR-210* promoter. When Su(Hw) was knocked down, no significant difference in the Dorsal signal was observed, indicating that Su(Hw) has no regulatory effect on the Dorsal signal in the *miR-210* promoter region (Figure 5E and F). These above findings suggested that infection-induced Dorsal promotes interaction with Su(Hw) to bind to the *miR-210* promoter and inhibit the expression of *miR-210* during the early stage of *Drosophila* Toll immune response.

## The Dorsal/Su(Hw)/*miR-210*/*Toll* regulatory loop contributes to *Drosophila* immune responses and homeostasis

To further explore the physiological role of the Dorsal/Su(Hw)/*miR-210*/Toll regulatory loop, we herein investigated the dynamic expression profiles of *Dorsal*, *su(Hw)*, *miR-210*, *Toll*, *Drs* in the wild-type (*w*$^{1118}$) flies at different time points (0, 0.5, 1, 2, 3, 6, 12, 24 and 48 h) after *M. luteus* infection, with PBS injection as control. Our results demonstrated that the expression level of *Drs* did not significantly change at 0∼0.5 h post-infection compared to the control group, but significantly increased at 1 h and peaked at 6 h post infection, then gradually decreased and returned to near initial level at 48 h after infection (Figure 6A). The expression level of *Dorsal* was significantly up-regulated at the early stages of infection, such as 0.5, 1 and 3 h post-infection (Figure 6B), while the expression level of *su(Hw)* was only significantly up-regulated at 2 h after infection (Figure 6C). Interestingly, the expression level of *miR-210* was significantly down-regulated at 2 and 3 h post-infection compared to the control group, but significantly up-regulated at 12 h post-infection, followed by a restoration to normal levels (Figure 6D). In contrast, the expression pattern of *Toll* was nearly opposite to that of *miR-210* during the early 1∼12 h response stages, especially at 2, 3 and 12 h post-infection

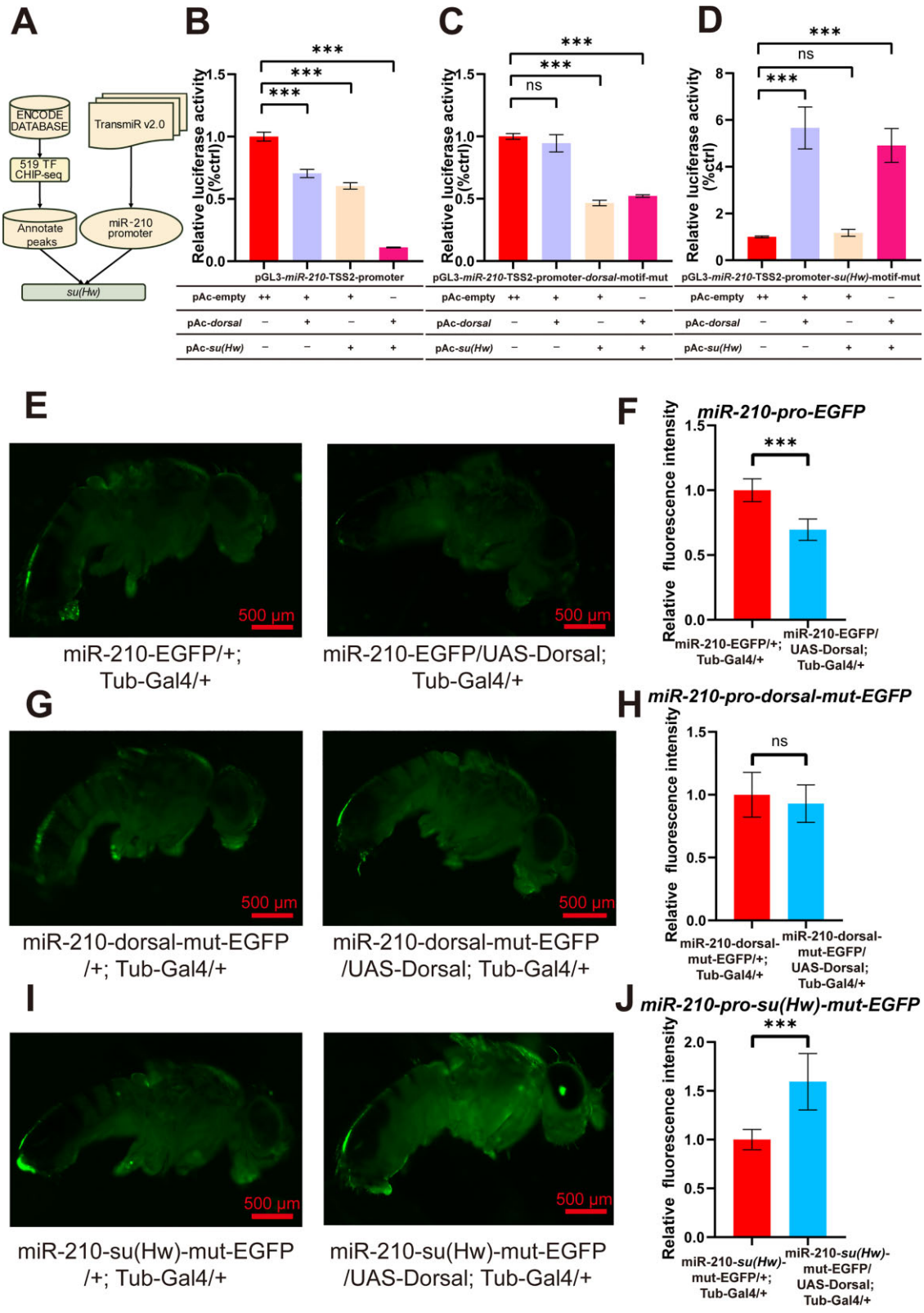


**Figure 4.** Dorsal-mediated transcriptional repression of *miR-210* depends on Su(Hw). (**A**) Flowchart illustrates the process of screening the transcription co-repressor Su(Hw) from the ENCODE database and TransmiR database. (**B–D**) The reporter activities of pGL3-*miR-210*-TSS2-promoter, the pGL3-*miR-210*-TSS2- promoter-*Dorsal*-motif-mut and the pGL3-*miR-210*-TSS2-promoter–*su(Hw)*-motif-mut were determined in *Drosophila* S2 cell using the luciferase assay, with exogenous Dorsal and Su(Hw) transfected separately or together. "+" indicated transfection with 500 ng of the plasmid, "++" indicated transfection with 1000 ng of the plasmid, "–" indicated no transfection of the plasmid. (**E**, **G**, **I**) Observation of *miR-210-EGFP*, *miR-210-Dorsal-mut-EGFP*, and *miR-210-su(Hw)-mut-EGFP* reporter gene fluorescence in control flies (left) and the *Dorsal* overexpressed flies (right) using a fluorescent microscope. (**F**, **H**, **J**) Quantification of EGFP intensity in the *miR-210-EGFP*, *miR-210-Dorsal-mut-EGFP* and *miR-210-su(Hw)-mut-EGFP* using imageJ (10 flies per group).

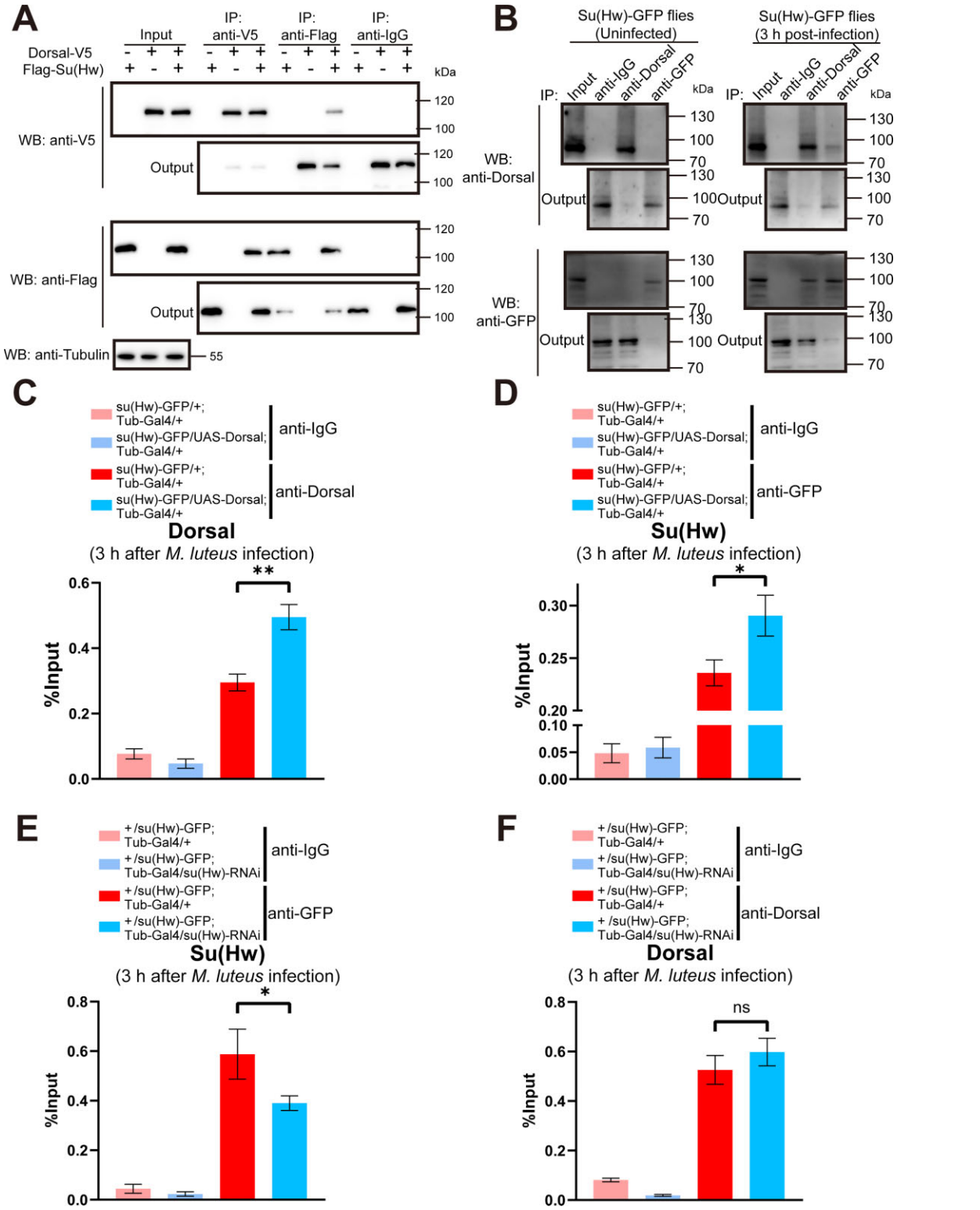


**Figure 5.** Infection-induced Dorsal interacts with Su(Hw) to suppress *miR-210* transcription. (**A**) *In vitro* Co-IP experiments were performed in S2 cells co-transfected with Dorsal-V5 and Flag-Su(Hw). Immunoprecipitation was performed using anti-V5 and anti-Flag antibodies, followed by western blot analysis with corresponding antibodies. (**B**) *In vivo* Co-IP experiments were conducted in Su(Hw)-GFP flies, both uninfected and at 3 h post-infection. Immunoprecipitation was performed using anti-Dorsal and anti-GFP antibodies, followed by western blot analysis with corresponding antibodies. (**C**) ChIP-qPCR analysis was performed in Su(Hw)-GFP flies with or without Dorsal overexpressed at 3 h post-infection to detect the fold change in Dorsal binding on the promoters of *miR-210*. (**D**) ChIP-qPCR analysis was performed in Su(Hw)-GFP flies with or without Dorsal overexpressed at 3 h post-infection to detect the fold change in Su(Hw) binding on the promoters of *miR-210*. (**E**) ChIP-qPCR analysis was performed in Su(Hw)-GFP flies with or without su(Hw) knocked down at 3 h post-infection to detect the fold change in Su(Hw) binding on the promoters of *miR-210*. (**F**) ChIP-qPCR analysis was performed in Su(Hw)-GFP flies with or without su(Hw) knocked down at 3 h post-infection to detect the fold change in Dorsal binding on the promoters of *miR-210*.

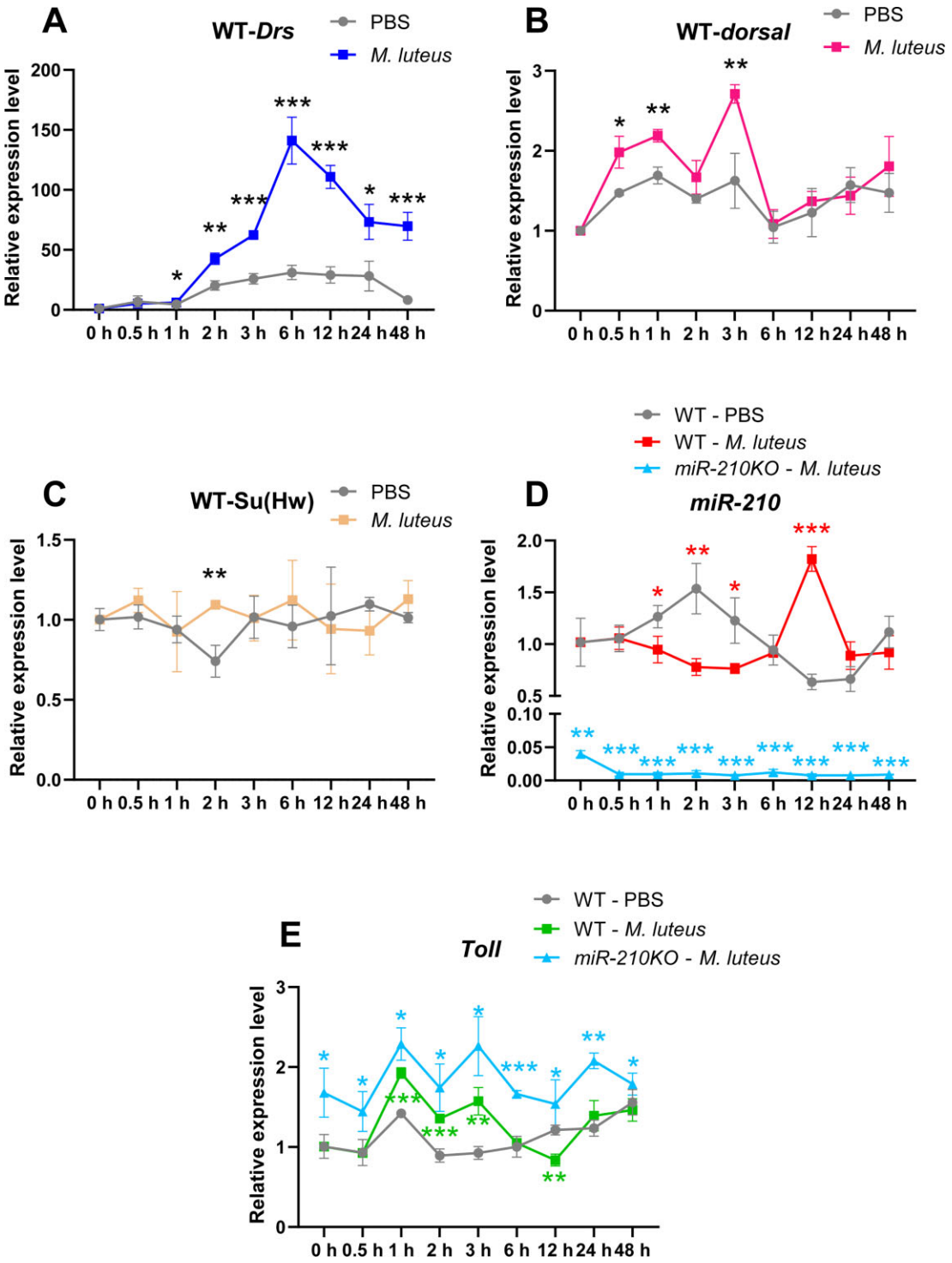


**Figure 6.** The Dorsal/Su(Hw)/*miR-210*/Toll regulation loop contributes to *Drosophila* Toll immune responses and homeostasis (**A**-**C**) The dynamic expressions of *Drs*, *Dorsal* and *su(Hw)* were detected by RT-qPCR in the wild-type ($w^{1118}$) *Drosophila* infected with *M. luteus* at 0, 0.5, 1, 2, 3, 6, 12, 24 and 48 h post-injection. (**D**) The dynamic expressions of *miR-210* in the wild-type ($w^{1118}$) and *miR-210KO* flies were detected by RT-qPCR at 0, 0.5, 1, 2, 3, 6, 12, 24 and 48 h post-infection. (**E**) The dynamic expressions of *Toll* in the wild-type ($w^{1118}$) and *miR-210KO* flies were detected by RT-qPCR at 0, 0.5, 1, 2, 3, 6, 12, 24 and 48 h post-infection.

(Figure 6E). Moreover, we examined the changes of *miR-210* and *Toll* expression in the *miR-210KO* flies at different times post-infection. Our results showed the expression level of *Toll* was remarkably enhanced in the *miR-210KO* flies compared to the WT flies at all time points post-infection, suggesting that *miR-210* may be primarily responsible for the change of *Toll* expression level (Figure 6D and E). Taken together, it is reasonable to speculate that in the early stage of *M. luteus* infection, the NF-κB transcription factor Dorsal interacted with Su(Hw) to form a complex to cooperatively inhibit *miR-210* transcription via binding to its promoter region, thereby up-regulating the expression level of target gene *Toll* as well as *Drs* to promote Toll pathway immune responses. Whilst in the late stage of *M. luteus* infection, these overexpressed AMPs may accompany the dissociation of the repressor complex of Dorsal and Su(Hw), resulting in the up-regulated expression of *miR-210* to suppress the *Toll* expression for reducing AMP expressions, thereby preventing the over-activation of Toll pathway immune response and restoring a new homeostasis (Figure 6). Therefore, our results revealed that the Dorsal/Su(Hw)/*miR-210*/*Toll* regulatory loop could contribute to *Drosophila* immune responses and homeostasis in a time- and dose-dependent manner.

## The *hsa-miR-210* targets and inhibits *TLR6* mRNA expression

Since *Drosophila miR-210* is homologous to human *hsa-miR-210* and *Toll* is homologous to human Toll-like receptor 6 (*TLR6*) from the DIOPT v8.0 database (Supplementary Figure S5A) (53,54), we herein wondered whether the above regulatory loop identified in flies also exists in human. The *TLR6* plays a crucial role in the immune response against G+ bacteria or yeast infections in human (55,56). We thus further validated the possible interaction between *TLR6* and *hsa-miR-210* using the miRWalk website (Supplementary Figure S5B), the dual luciferase reporter and RIP-qPCR assays. Our results demonstrated that the mimics-*hsa-miR-210* significantly inhibited the luciferase activity of the reporter containing the 3' UTR of *TLR6* (∼4 kb) compared to the control group (mimics-NC), while the point mutation in the 3' UTR of *TLR6* disrupted the inhibition effect (Figures 7A and B). Interestingly, the RIP-qPCR experiments demonstrated that the *TLR6* RNA immunoprecipitated by anti-Ago2 was increased nearly ten-fold after transfection with mimics-*hsa-miR-210* compared to the control group (mimics-NC) in THP1-induced macrophages (Figures 7C). These results revealed that *hsa-miR-210* could bind directly to the 3' UTR of *TLR6* and inhibit its expression.

## RelA-mediaded transcriptional inhibition of *hsa-miR-210* depends on E4F1

Phylogenetic analysis demonstrated that among the five human NF-κB family transcription factors, RelA, Rel and RelB have higher homology with *Drosophila* Dorsal (Supplementary Figure S6A). The further bioinformatics analysis found that the RelA has binding motif in the promoter region of *hsa-miR-210* using TransmiR, PROMO and JASPAR database (Figures 7D and Supplementary Figure S5C–E). We thus examined the effect of RelA on the activity of the *hsa-miR-210* promoter (*hsa-miR-210*-promoter) based on the TSS annotation of the *hsa-miR-210* from miRGen v.3 database (57), with the reverse strand sequence of the *hsa-miR-210* promoter (*hsa-miR-210*-promoter-AS) as a negative control. Our results showed that only the *hsa-miR-210* promoter sequence had luciferase activity in human 293T cells, while the *hsa-miR-210*-promoter-AS had no promoter activity (Figures 7D and E). Especially, the inhibitory intensity of RelA on the *hsa-miR-210* promoter activity increased with the increase of RelA plasmid concentrations and protein levels (Supplementary Figure S6B), which was consistent with these results of *Drosophila* in a dosage dependent manner (Supplementary Figure S4E).

We found that human E4F1 and ZNF358 as well as *Drosophila* Su(Hw) are all members of zinc finger protein family via the DIOPT v8.0 database, implying that human E4F1 and ZNF358 may have similar function with *Drosophila* Su(Hw) (Supplementary Figure S5F). Interestingly, we found that E4F1 has the binding motif in the promoter region of *hsa-miR-210* (Figures 7D and Supplementary Figure S5G). Similar to *Drosophila* Su(Hw), E4F1 exhibited a more significant inhibitory effect on the promoter activity of *hsa-miR-210* than RelA, and this inhibitory effect was also concentration-dependent (Supplementary Figure S6C). However, ZNF358 failed to inhibit the promoter activity of *hsa-miR-210* and was served as a negative control (Supplementary Figure S6E). To further validate the regulatory pattern of RelA and E4F1 on the *hsa-miR-210* promoter, we examined the activity of the *hsa-miR-210* promoter after transfection with cmv-Flag-*RelA* and pcDNA3.0-HA-*E4F1* alone or simultaneously, and found that the co-transfection of RelA and E4F1 exhibits stronger cooperative repression on the *hsa-miR-210* promoter compared to their individual transfection (Figures 7F and Supplementary Figure S6F), which further supports the cooperative inhibitory function between these two factors. We further mutated the binding motifs of RelA and E4F1 in the promoter region of *hsa-miR-210*, and then transfected Flag-RelA and HA-E4F1 alone or simultaneously, finding that the mutation of the RelA motif did not affect the repression of E4F1 on the promoter activity of *hsa-miR-210*, but the regulation of RelA on *hsa-miR-210* changed from inhibition to activation when the E4F1 motif was mutated (Figures 7G and H), which was similar to the regulation pattern of *Drosophila* Dorsal and Su(Hw) on the *miR-210* promoter (Figure 4B-D). Our results revealed that RelA-mediated transcriptional repression of *hsa-miR-210* is dependent on E4F1.

## NF-κB/RelA interacts with E4F1 to suppress *hsa-miR-210* transcription

Here, we further performed *in vitro* Co-IP experiments in 293T cells after transfecting CMV-3xFlag-*RelA* and pcDNA3.0-HA-*E4F1* plasmids alone or simultaneously, and found that the Flag-RelA could be clearly detected after immunoprecipitation using anti-HA in 293T cells transfected with CMV-3xFlag-*RelA* and pcDNA3.0-HA-*E4F1*, and the same for the HA-E4F1 (Figure 8A, quantified in Supplementary Figure S7E and F). Especially, we found that under non-infected condition, there was no interaction between RelA and E4F1 in THP1-induced macrophages through the *in vivo* Co-IP assay using antibodies against RelA and E4F1 (Figure 8B). Interestingly, a clear interaction between RelA and E4F1 was observed at 0.5 h post-infection, suggesting that the interaction between RelA and E4F1 could be induced by infection (Figure 8B, quantified in

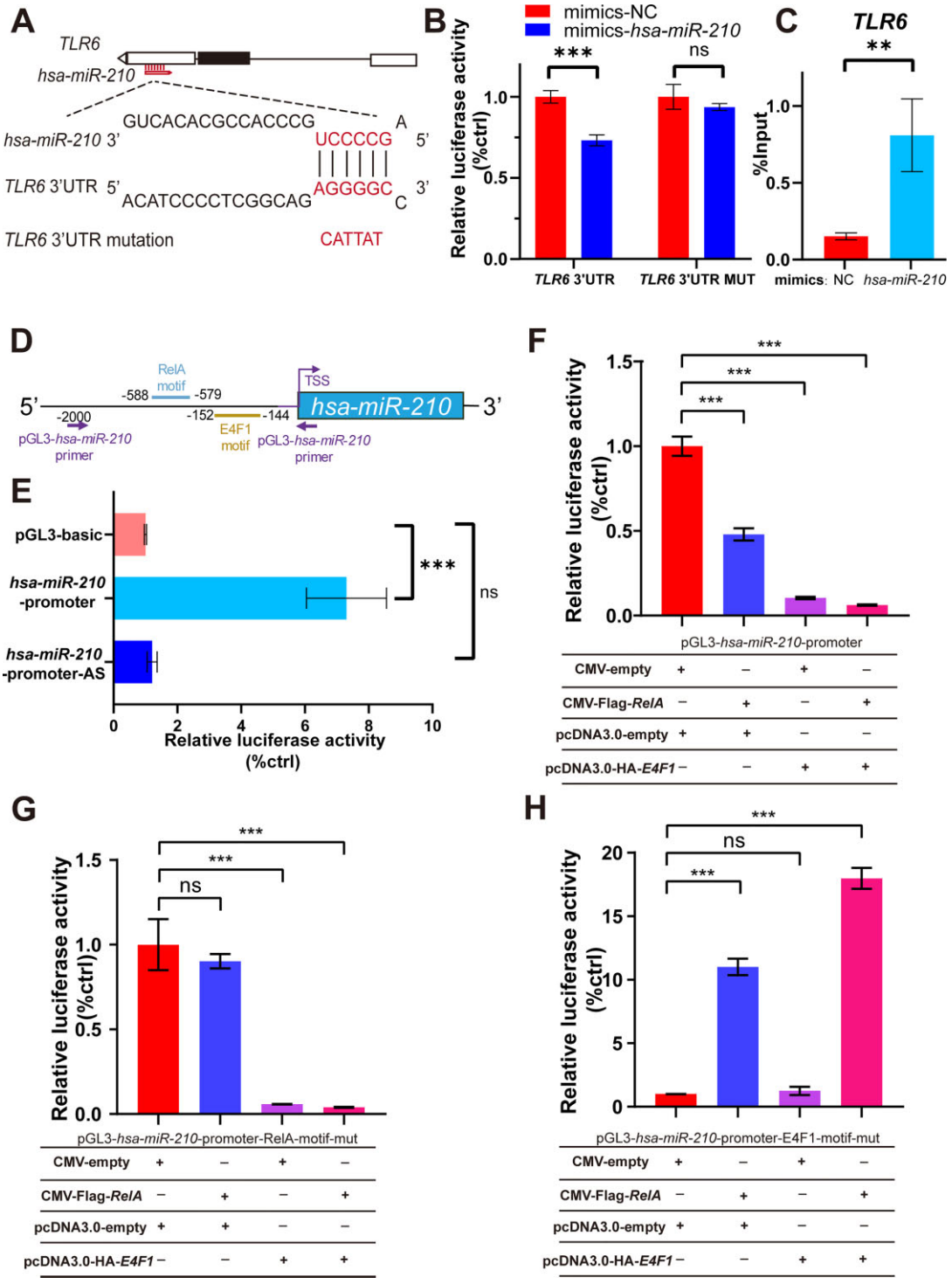


**Figure 7.** *hsa-miR-210* directly targets *TLR6* and RelA-mediated transcriptional repression of *hsa-miR-210* depends on E4F1. (**A**) Potential binding sites of *hsa-miR-210* in 3'UTR region of *TLR6* were predicted using the miRWalk website. Point mutations were introduced at the target site in the 3'UTR, which resulted in base-pairing with the seed sequence of *hsa-miR-210*. (**B**) Dual luciferase assay was performed in 293T cells to determine the luciferase activities of mimics-*hsa-miR-210* and a reporter plasmid with or without the mutation site of target *TLR6*. (**C**) RIP-qPCR experiment was performed in THP1-induced macrophages transfected with mimics-NC or mimics-*hsa-miR-210,* using anti-Ago2 antibody. (**D**) Schematic diagram illustrates the promoter region of *hsa-miR-210*. The predicted TSS, position of the designed primer (purple line), RelA motifs (blue line) and E4F1 motifs (orange line) were marked. (**E**) Luciferase assay was performed in 293T cells to determine the activity of *pGL3-hsa-miR-210-promoter* and the *pGL3-hsa-miR-210-promoter-AS* reporters. (**F**) Luciferase assay was performed in 293T cells to determine the activity of the pGL3-*hsa-miR-210*-promoter reporters. Exogenous RelA and E4F1 were separately or jointly included in the assay. "+" indicated transfection with 500 ng of this plasmid, "–" indicated no transfection of the plasmid in 293T cells. (**G**) Luciferase assay was performed in 293T cells to determine the activity of the pGL3-*hsa-miR-210*-promoter-RelA-motif-mut reporters. Exogenous RelA and E4F1 were separately or jointly included in the assay. "+" indicated transfection with 500 ng of this plasmid, "–" indicated no transfection of the plasmid in 293T cells. (**H**) Luciferase assay was performed in 293T cells to determine the activity of the pGL3-*hsa-miR-210*-promoter-E4F1-motif-mut reporters. Exogenous RelA and E4F1 were separately or jointly included in the assay. "+" indicated transfection with 500 ng of this plasmid, "–" indicated no transfection of the plasmid in 293T cells.

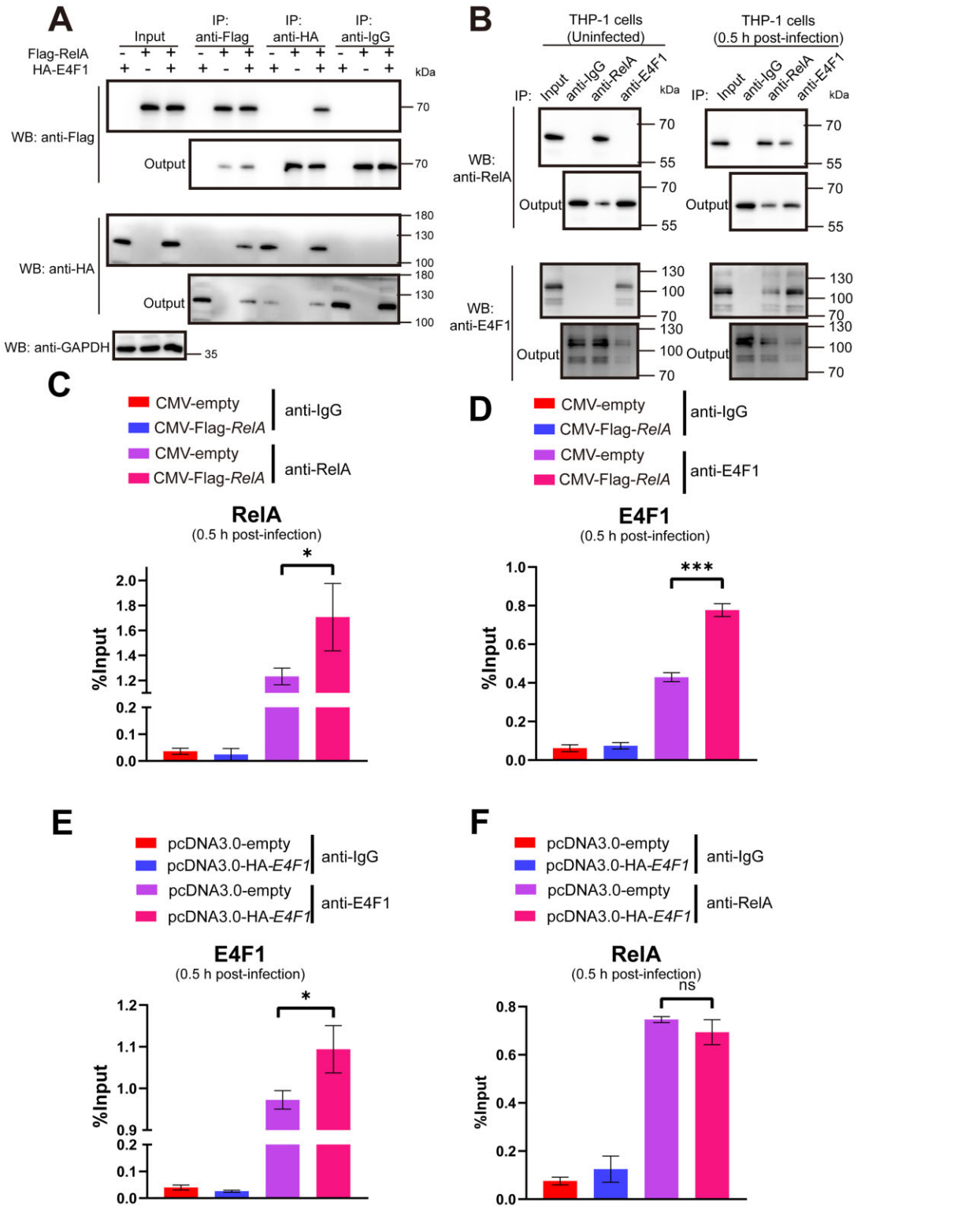


**Figure 8.** Interaction between RelA and E4F1 suppresses *hsa-miR-210* transcription in the early stage of G+ bacterial stimulation. (**A**) *In vitro* Co-IP experiments were performed in 293T cells co-transfected with Flag-RelA and HA-E4F1 using anti-Flag and anti-HA antibodies for immunoprecipitation, followed by western blot analysis using corresponding antibodies. (**B**) *In vivo* Co-IP experiments were performed in THP1-induced macrophages, both uninfected and at 0.5 h post-infection, using anti-RelA, anti-E4F1 antibodies for immunoprecipitation, followed by western blot analysis using corresponding antibodies. (**C**) ChIP-qPCR was performed in THP1-induced macrophages, with and without overexpression of RelA at 0.5 h post-infection, to detect fold change on the promoters of *hsa-miR-210* using anti-RelA antibodies for the immunoprecipitation *in vivo*. (**D**) ChIP-qPCR was performed in THP1-induced macrophages, with and without overexpression of RelA at 0.5 h post-infection, to detect fold change on the promoters of *hsa-miR-210* using anti-E4F1 antibodies for the immunoprecipitation *in vivo*. (**E**) ChIP-qPCR was performed in THP1-induced macrophages, with and without overexpression of E4F1 at 0.5 h post-infection, to detect fold change on the promoters of *hsa-miR-210* using anti-E4F1 antibodies for the immunoprecipitation *in vivo*. (**F**) ChIP-qPCR was performed in THP1-induced macrophages, with and without overexpression of E4F1 at 0.5 h post-infection, to detect fold change on the promoters of *hsa-miR-210* using anti-RelA antibodies for the immunoprecipitation *in vivo*.

Supplementary Figure S7G and H). These results are consistent with the interaction pattern between *Drosophila* Dorsal and Su(Hw), which suggests that the interaction of infection-induced NF-κB factors with zinc finger protein Su(Hw)/E4F1 is conserved in *Drosophila* and human.

We further overexpressed RelA and E4F1 separately in THP1-induced macrophages at 0.5 h post-infection and examined the signals of RelA and E4F1 in the *miR-210* promoter region using anti-RelA and anti-E4F1 antibodies. Our results demonstrated that the overexpression of RelA increased its signal in the *hsa-miR-210* promoter region, which was accompanied by a significant increase of E4F1 signal in the *hsa-miR-210* promoter region, suggesting that RelA could interact with E4F1 to bind to the *hsa-miR-210* promoter region post-infection (Figure 8C and D). On the contrary, no difference was observed in the signal of RelA after the overexpression of E4F1, indicating that E4F1 has no regulatory effect on RelA signal in the promoter region of *hsa-miR-210* (Figure 8E and F). Our findings revealed a highly conserved mechanism in which infection-induced NF-κB factors can promote the interaction with zinc finger protein Su(Hw)/E4F1 and bind to the *miR-210* promoter, thereby leading to the inhibition of *miR-210* expression in *Drosophila* and human in the early stage of G+ bacterial stimulation.

### The role of the RelA/E4F1/*hsa-miR-210*/*TLR6* regulatory loop in THP1-induced macrophages

We herein used THP1-induced macrophages to further detect the role of the RelA/E4F1/*hsa-miR-210*/*TLR6* regulatory loop. Our results demonstrated that the transfection of mimics-*hsa-miR-210* into the THP1-induced macrophages could significantly down-regulate the expression of downstream immune factors (*IFNB*, *IL6* and *TNFA*) of human TLR signaling pathway compared to that of the mimics-NC control at 3 h after stimulation with the heat-killed G+ bacteria *M. luteus* (Figure 9A), indicating that *hsa-miR-210* plays a critical role in human innate immune response. Of note, the levels of both RNA and protein of *TLR6*, the *hsa-miR-210* target gene, in THP1-induced macrophages were significantly declined compared to the mimics-NC control (Figure 9B and C). Especially, we also examined the expression levels of *RelA*, *E4F1*, *hsa-miR-210,* and *TLR6* in THP1-induced macrophages at various time points (0, 0.25, 0.5, 1, 2 and 3 h) after infection with heat-killed *M. luteus*, and demonstrated that the level of E4F1 protein was significantly increased by approximately 30% at 0.5 h post-infection compared to the control group, and subsequently decreased by about 50–60% at 2–3 h after immune stimulation (Figure 9D and E). Meanwhile, the expression level of phosphorylated-RelA protein was observably increased compared to the control groups at 0.5–3 h post-infection (Figure 9D and F). In contrast, the expression level of *hsa-miR-210* was significantly decreased in the early stage of immune response (0.5 h) and increased significantly in the later stage (3 h) compared to the control group (Figure 9G). Moreover, the expression level of *TLR6* exhibited an opposite pattern to *hsa-miR-210* (Figure 9H). To further confirm the association between changes in *hsa-miR-210* and *TLR6* expression post-infection, we monitored the expression changes of *hsa-miR-210* and *TLR6* in THP1-induced macrophages transfected with inhibitor-*hsa-miR-210* at different times post-infection. The results revealed that the expression level of *TLR6* was increased significantly in THP1-induced macrophages transfected with inhibitor-*hsa-miR-210* compared to that transfected with inhibitor-NC post-infection, suggesting that *hsa-miR-210* may be primarily responsible for the change of *TLR6* expression post-infection (Figure 9G and H). Taken together, our results revealed that the RelA/E4F1/*hsa-miR-210*/*TLR6* regulatory loop can contribute to human immune responses and homeostasis in a time- and dose-dependent manner in the THP1-induced macrophages after infection, which is similar to that in *Drosophila*.

## Discussion

The tight control of immune response duration and strength is crucial for effective host defense. Although miRNAs have been demonstrated to play crucial roles in fine-tuning immune signals, the dynamic regulations of immune-specific miRNAs themselves remains poorly understood (58,59). In this study, we aimed to investigate how one conserved *miR-210* regulates and is regulated in innate immune response to G+ bacterial stimulation. Our findings contribute to a better understanding of the regulation by and of immune-specific miRNAs.

The *miR-210* is evolutionarily conserved between *Drosophila* and mammals (60), and has been involved in the regulation of photoreceptor neurons, circadian rhythms and lipid metabolism in *Drosophila* (42,61,62). However, its role in immune response remains unknown. In our work, we revealed that *miR-210* can negatively regulate *Drosophila* Toll signaling via directly repressing the expression of target gene *Toll* (Figure 1). Interestingly, a similar regulatory relationship was also found in the human TLR signaling pathway (Figures 7 and 9). In contrast to *Drosophila*, the human *hsa-miR-210* can extensively regulate a variety of biological processes, including inflammation, cell cycle, DNA damage repair, apoptosis, particularly the occurrence and development of cancer (63,64). However, little is known about the transcriptional activation and regulation of *miR-210* itself in *Drosophila* and human. Mounting studies have focused on the regulatory roles of miRNAs, but little attention has been paid to how these miRNAs themselves are regulated, especially at transcriptional level. Interestingly, several studies have revealed that the dynamic and specific expressions of miRNAs can be precisely controlled by transcription factors (15,65,66). For instance, in mammals, the Hypoxia Inducible Factor-1 (HIF-1) acts as a principal transcription factor that binds to the *miR-210* promoter and activates *miR-210* transcription in response to hypoxia (67). Other transcription factors such as Oct-4, AP2, PPARc, and E2F have been reported to bind to the *miR-210* promoter regions, although their regulatory roles remain unclear (68). These studies suggest that the multifunctional roles of *miR-210* might be precisely regulated via different transcription factors. Similarly, the NF-κB family transcription factors are essential for innate immune response, whether they can also control the transcription of *miR-210* to involve in innate immune response? Herein, we have provided compelling evidences that NF-κB counterparts from *Drosophila* Toll and human TLR signaling pathways regulate *miR-210* expression. Specifically, we demonstrated that *Drosophila* NF-κB/Dorsal inhibits *miR-210* transcriptional activity via binding to its promoter region (Figure 2). To ensure accuracy, the enhancement of positive control *Drs* expression was also detected when overexpressing Dorsal *in vitro* and *in vivo,* which is

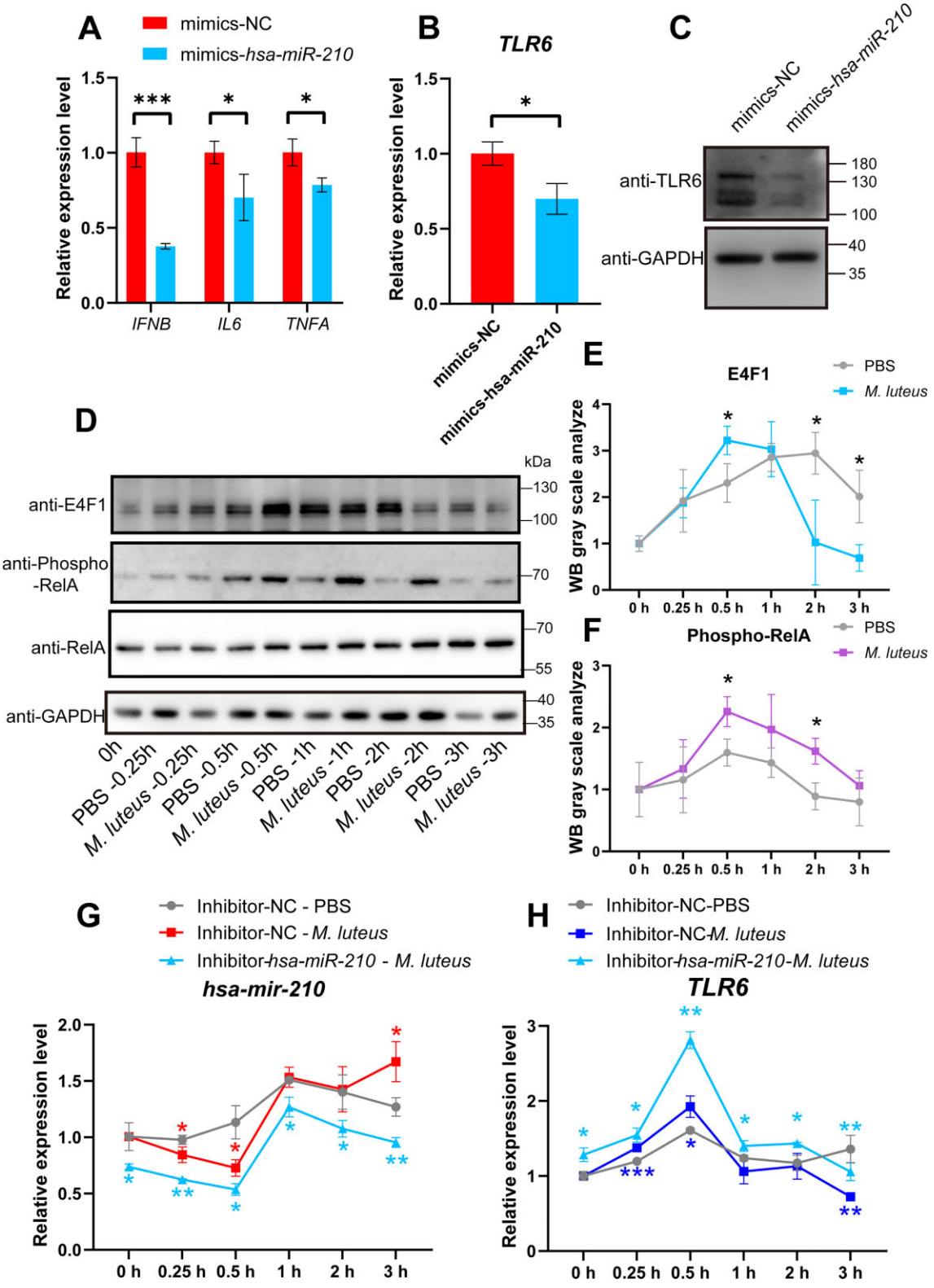


**Figure 9.** The RelA/E4F1/*hsa-miR-210*/*TLR6* regulation loop contributes to innate immune responses in THP1-induced macrophages. (**A**) RT-qPCR analysis of *IFNB*, *IL6* and *TNFA* expression was measured in THP1-induced macrophages transfected with mimics-NC or mimics-*hsa-miR-210* and stimulated with heat-killed *M. luteus* [multiplicity of infection (MOI) = 50]. (**B**) RT-qPCR analysis of *TLR6* expression was measured in THP1-induced macrophages transfected with mimics-NC or mimics-*hsa-miR-210* and stimulated with heat-killed *M. luteus* [multiplicity of infection (MOI) = 50]. (**C**) Changes in the protein levels of TLR6 were assessed in THP1-induced macrophages with mimics-NC or mimics-*hsa-miR-210* transfection and heat-killed *M. luteus* [multiplicity of infection (MOI) = 50] stimulated. (**D**) Changes in the protein levels of E4F1, Phospho-RelA, RelA and GAPDH were analyzed in THP1-induced macrophages using western blot at different time points post-infection. (**E**) Western blot grayscale analysis of E4F1 in THP1-induced macrophages at different time points post-infection. (**F**) Western blot grayscale analysis of Phospho-RelA in THP1-induced macrophages at different time points post-infection. (**G**) The dynamic expressions of *hsa-miR-210* in THP1-induced macrophages transfected with inhibitor-NC and inhibitor-*hsa-miR-210* were detected by RT-qPCR at 0, 0.25, 0.5, 1, 2, 3 h post-infection. (**H**) The dynamic expressions of *TLR6* in THP1-induced macrophages transfected with inhibitor-NC and inhibitor-*hsa-miR-210* were detected by RT-qPCR at 0, 0.25, 0.5, 1, 2, 3 h post-infection.

consistent with the previous report (69) (Figure 2). Of great importance, we also demonstrate that the human NF-κB family transcription factor RelA represses the transcription of *hsa-miR-210* via binding to its promoter region (Figure 7), revealing an evolutionarily conserved mechanism between *Drosophila* and human. Overall, our study suggests that specific expression of *miR-210* in *Drosophila* and human can be precisely regulated by NF-κB transcription factors, thereby performing critical immune regulation roles.

Currently, NF-κB factors are primarily considered to execute transcriptional activation functions on antimicrobial peptides in insects and downstream cytokines in human via its transactivation domain (TAD). For example, human RelA can activate *miR-34a* via directly binding to its promoter, thereby inhibiting Foxp3 expression involved in the regulatory of T cells (65). However, another study reported that RelA can inhibit *miR-30a* transcription to regulate Th17 differentiation (70), but its transcriptional inhibition mechanism has not been further investigated. We thus speculated that the inhibition of *miR-210* by NF-κB factors may need to interact with transcriptional repressors. Interestingly, our work demonstrated that *Drosophila* zinc finger protein Su(Hw) can serve as a transcriptional repressor by binding to and inhibiting the promoter of *miR-210* (Figure 4). Previous studies have indicated that Su(Hw) protein not only acts as a chromatin insulator (71), but also forms transcriptional inhibitory complexes with other proteins (22,72,73). Consistently, our present study has demonstrated that infection-induced Dorsal interacted with Su(Hw) to form a complex and further inhibit *miR-210* transcription by binding to its promoter region during the early stage of *M. luteus* infection (Figure 4 and 5). Remarkably, the co-overexpression of Dorsal and Su(Hw) has a significantly stronger inhibitory effect on the promoter activity of *miR-210* compared to their individual overexpression (Figure 4B). Overexpressing Su(Hw) can still significantly inhibit the promoter activity of *miR-210* even with Dorsal motif mutation on *miR-210* promoter (Figure 4C), whereas overexpressing Dorsal can promote transcriptional activation of *miR-210* following Su(Hw) motif mutation on *miR-210* promoter (Figure 4D, I and J). These results suggested that the Dorsal-mediated inhibition on *miR-210* promoter is dependent on Su(Hw). Furthermore, our study demonstrated that infection-induced Dorsal can interact with more Su(Hw) to enhance the Su(Hw) signal on *miR-210* promoter during the early stage (3 h) of Toll pathway immune response (Figure 5C and D). Our work reveals a novel immunomodulatory mechanism by which Dorsal suppresses *miR-210* expression via interacting with Su(Hw) to enhance immune response during the early stage response to G+ bacterial stimulation in *Drosophila*. Meanwhile, another *Drosophila* NF-κB factor Dif can also inhibit the expression of *miR-210* and interact with Su(Hw) *in vitro*, suggesting this immunomodulatory mechanism might be conserved among different NF-κB factors (Supplementary Figure S8).

However, it is worth noting that the interaction between transcription factors and their associated protein complexes is complex and often involves multiple partners and regulatory mechanisms. Although we have performed *in vivo* and *in vitro* Co-IP experiments between Dorsal and Su(Hw) to yield positive results in this study, this does not exclude the possibility of Dorsal interacting with the other compositions of the Su(Hw) complex to form the complex because Su(Hw) can also exert a positive effect on the transcription from nearby promoters (74,75) and its main partners Mod(mdg4) and CP190 are not known as suppressor proteins (76–79), implying that Dorsal may also need to stabilize/recruit other repressed complex at the Su(Hw) site in the *miR-210* promoter to inhibit its expression. Therefore, further investigations on the other compositions of the complex besides Dorsal and Su(Hw) are needed to fully elucidate the dynamic expression mechanism of *miR-210*.

Strikingly, we have identified a human zinc-finger protein E4F1, which may perform a similar function to *Drosophila* Su(Hw). Although E4F1 as transcription repressor has been reported to be involved in stem cell homeostasis (80–82), ROS-mediated death in human myeloid leukemia cell lines (83,84) and DNA double-strand break repair (85), its regulatory role in innate immune responses has not yet been reported to date. In our study, we discovered that in the early stage of G+ bacterial stimulation, the protein levels of E4F1 are significantly up-regulated in the THP1-induced macrophages (Figure 9D and E). Especially, we found that RelA can interact with E4F1 to form a transcriptional inhibitory complex, thereby leading to the inhibition of *hsa-miR-210* expression via binding to its promoter region (Figure 7 and 8). Notably, E4F1 has a more significant inhibitory effect on the activity of *hsa-miR-210* promoter than RelA (Figure 7F and G). Similar to *Drosophila* Dorsal and Su(Hw), the binding motif of E4F1 is closer to the TSS site of *hsa-miR-210* than RelA (Figure 7D). Of note, in this work, the level of inhibition on *hsa-miR-210* promoter activity was very similar between the plasmid transfected with pcDNA3.0-HA-*E4F1* (500 ng) + cmv-empty (500 ng) and the plasmid transfected with pcDNA3.0-HA-*E4F1* (500 ng) + cmv-Flag-*RelA* (500 ng) (Figure 7F). This is probably because the levels of E4F1 plasmid being transfected in these experiments is too high. We thus repeated the experiment via reducing the plasmid levels of E4F1 and RelA by half (250 ng), and found that the co-transfection of RelA and E4F1 exhibited a stronger cooperative repression on the *hsa-miR-210* promoter activity compared to their individual transfection, which further supported the cooperative inhibitory function between the two factors (Supplementary Figure S6F). Together, our work suggests that the regulation mechanism of NF-κB family transcription factors interacting with transcriptional repressors to inhibit *miR-210* expression is evolutionarily conserved between *Drosophila* and human innate immune responses. In our work, the protein level of E4F1 is decreased, but the level of phosphorylated-RelA remains increased compared to the controls in the late stage of infection, indicating that the transition from transcriptional repression to reactivation of *miR-210* may be due to the dissociation of the inhibitory complex or potential degradation of repressors.

Fascinatingly, our work demonstrated a tightly coordinated dynamic expression profile of *Dorsal*, *su(Hw)*, *miR-210*, *Toll,* and *Drs* in the wild-type ($w^{1118}$) flies upon infection, as well as *RelA*, *E4F1*, *hsa-miR-210* and *TLR6* in the THP1-induced macrophage with infection, suggesting that animal innate immune responses can be finely regulated in a time- and dose-dependent manner (Figures 6 and 9). Therefore, we herein proposed an evolutionary conservative regulatory mechanism for maintaining innate immune homeostasis (Graphical Abstract). On the one hand, to prevent inadequate immune responses in the early stage of pathogen infection, the NF-κB family transcription factors (e.g. *Drosophila* Dorsal and human RelA) interact with transcription repressors (e.g. *Drosophila* Su(Hw) and human E4F1) at the appropriate time to form a complex and bind to the promoter region

of *miR-210*, and inhibit *miR-210* expression to de-suppress target gene *Toll/TLR6*, thereby enhancing immune response to eliminate invading pathogenic bacteria. On the other hand, with the continuous enhancement of immune response, the complexes containing Dorsal and Su(Hw) or RelA and E4F1 are dissociated with progressively decreased repressors to restore the *miR-210* expression, thereby further inhibiting the expression of target gene *Toll/TLR6* to prevent the excessive immune response and maintain a new immune homeostasis in the late stages of pathogen infections (Graphical Abstract). Mechanistically, our work sheds light on a novel conserved regulatory mechanism of immune responses between invertebrate and mammal.

## Conclusion

In this work, we have identified *miR-210* and Su(Hw) as new regulators in the *Drosophila* Toll pathway, along with E4F1 and *hsa-miR-210* as new regulators in the human TLR pathway. We have also demonstrated that NF-κB factors (Dorsal in *Drosophila* and RelA in human) control *miR-210* expression via interacting with transcription repressors (Su(Hw) in *Drosophila* and E4F1 in human) in a time- and dose-dependent manner. More importantly, we have elucidated a conserved regulatory mechanism for innate immune response and immune homeostasis in the *Drosophila* Toll and human TLR signaling pathways. Our study not only unveils a conserved TFs/*miR-210*/targets regulatory loop in both *Drosophila* and human, but also provides vital insights into the dynamic regulation of miRNA expression during animal innate immune responses.

## Data availability

The data underlying this article are available in the article and in its online supplementary material. Further data underlying this article will be shared on reasonable request to the corresponding author.

## Supplementary data

Supplementary Data are available at NAR Online.

## Acknowledgements

We would like to thank Bloomington, FlyORF for fly stocks, Professor Liming Chen from Nanjing Normal University and Associate Professor Yao Li from Yangzhou University for discussing on ideas and experimental designing, Qidong Fungene Biotechnology (http://www.fungene.tech) for EGFP flies construction.

## Funding

National Natural Science Foundation of China [32370516 to F.M., 31970477 to F.M., 32370515 to P.J., 32300401 to H.Z.]; Natural Science Foundation from Jiangsu Province [BK20231282 to P.J.]; Project Funded by the Priority Academic Program Development of Jiangsu Higher Education Institutions and Jiangsu Funding Program for Excellent Postdoctoral Talent (to H.Z.). Funding for open access charge: National Natural Science Foundation of China [32370516, 31970477, 32370515, 32300401].

## Conflict of interest statement

None declared.

## References

1. Hoffmann,J.A. (2003) The immune response of Drosophila. *Nature*, **426**, 33–38.
2. Belvin,M.P. and Anderson,K.V. (1996) A conserved signaling pathway: the drosophila toll-dorsal pathway. *Annu. Rev. Cell Dev. Biol.*, **12**, 393–416.
3. Valanne,S., Wang,J.H. and Ramet,M. (2011) The Drosophila Toll signaling pathway. *J. Immunol.*, **186**, 649–656.
4. Tanji,T. and Ip,Y.T. (2005) Regulators of the toll and Imd pathways in the Drosophila innate immune response. *Trends Immunol.*, **26**, 193–198.
5. He,X., Yu,J., Wang,M., Cheng,Y., Han,Y., Yang,S., Shi,G., Sun,L., Fang,Y., Gong,S.T., *et al.* (2017) Bap180/Baf180 is required to maintain homeostasis of intestinal innate immune response in Drosophila and mice. *Nat. Microbiol.*, **2**, 17056.
6. Ragab,A., Buechling,T., Gesellchen,V., Spirohn,K., Boettcher,A.L. and Boutros,M. (2011) Drosophila Ras/MAPK signalling regulates innate immune responses in immune and intestinal stem cells. *EMBO J.*, **30**, 1123–1136.
7. Aggarwal,K. and Silverman,N. (2008) Positive and negative regulation of the Drosophila immune response. *BMB Rep.*, **41**, 267–277.
8. Valanne,S., Vesala,L., Maasdorp,M.K., Salminen,T.S. and Ramet,M. (2022) The Drosophila toll pathway in Innate immunity: from the core pathway toward effector functions. *J. Immunol.*, **209**, 1817–1825.
9. Bartel,D.P. (2009) MicroRNAs: target recognition and regulatory functions. *Cell*, **136**, 215–233.
10. Lee,G.J. and Hyun,S. (2014) Multiple targets of the microRNA miR-8 contribute to immune homeostasis in Drosophila. *Dev. Comp. Immunol.*, **45**, 245–251.
11. Li,S., Xu,J., Sun,L., Li,R., Jin,P. and Ma,F. (2017) Drosophila miR-964 modulates toll signaling pathway in response to bacterial infection. *Dev. Comp. Immunol.*, **77**, 252–258.
12. Li,S., Li,Y., Shen,L., Jin,P., Chen,L. and Ma,F. (2017) miR-958 inhibits Toll signaling and drosomycin expression via direct targeting of toll and Dif in drosophila melanogaster. *Am. J. Physiol. Cell Physiol.*, **312**, C103–C110.
13. Li,R., Huang,Y., Zhang,Q., Zhou,H., Jin,P. and Ma,F. (2019) The miR-317 functions as a negative regulator of toll immune response and influences Drosophila survival. *Dev. Comp. Immunol.*, **95**, 19–27.
14. Li,R., Yao,X., Zhou,H., Jin,P. and Ma,F. (2021) The drosophila miR-959-962 cluster members repress toll signaling to regulate antibacterial defense during bacterial infection. *Int. J. Mol. Sci.*, 22.
15. Krol,J., Loedige,I. and Filipowicz,W. (2010) The widespread regulation of microRNA biogenesis, function and decay. *Nat. Rev. Genet.*, **11**, 597–610.
16. Zhou,R., Hu,G., Gong,A.Y. and Chen,X.M. (2010) Binding of NF-kappaB p65 subunit to the promoter elements is involved in LPS-induced transactivation of miRNA genes in human biliary epithelial cells. *Nucleic Acids Res.*, **38**, 3222–3232.
17. Hetru,C. and Hoffmann,J.A. (2009) NF-kappaB in the immune response of Drosophila. *Cold Spring Harb. Perspect. Biol.*, **1**, a000232.
18. Parkhurst,S.M., Harrison,D.A., Remington,M.P., Spana,C., Kelley,R.L., Coyne,R.S. and Corces,V.G. (1988) The Drosophila su(Hw) gene, which controls the phenotypic effect of the gypsy transposable element, encodes a putative DNA-binding protein. *Genes Dev.*, **2**, 1205–1215.
19. Gerasimova,T.I., Gdula,D.A., Gerasimov,D.V., Simonova,O. and Corces,V.G. (1995) A Drosophila protein that imparts directionality on a chromatin insulator is an enhancer of position-effect variegation. *Cell*, **82**, 587–597.

20. Holdridge,C. and Dorsett,D. (1991) Repression of hsp70 heat shock gene transcription by the suppressor of hairy-wing protein of Drosophila melanogaster. *Mol. Cell. Biol.*, **11**, 1894–1900.
21. Spana,C., Harrison,D.A. and Corces,V.G. (1988) The Drosophila melanogaster suppressor of Hairy-wing protein binds to specific sequences of the gypsy retrotransposon. *Genes Dev.*, **2**, 1414–1423.
22. Melnikova,L., Elizar'ev,P., Erokhin,M., Molodina,V., Chetverina,D., Kostyuchenko,M., Georgiev,P. and Golovnin,A. (2019) The same domain of Su(Hw) is required for enhancer blocking and direct promoter repression. *Sci. Rep.*, **9**, 5314.
23. Duan,T. and Geyer,P.K. (2018) Spermiogenesis and male fertility require the function of suppressor of hairy-wing in somatic cyst cells of drosophila. *Genetics*, **209**, 757–772.
24. Soshnev,A.A., Baxley,R.M., Manak,J.R., Tan,K. and Geyer,P.K. (2013) The insulator protein suppressor of Hairy-wing is an essential transcriptional repressor in the drosophila ovary. *Development*, **140**, 3613–3623.
25. Lambert,S.A., Jolma,A., Campitelli,L.F., Das,P.K., Yin,Y., Albu,M., Chen,X., Taipale,J., Hughes,T.R. and Weirauch,M.T. (2018) The Human transcription factors. *Cell*, **172**, 650–665.
26. Reiter,F., Wienerroither,S. and Stark,A. (2017) Combinatorial function of transcription factors and cofactors. *Curr. Opin. Genet. Dev.*, **43**, 73–81.
27. Wang,H., Garzon,R., Sun,H., Ladner,K.J., Singh,R., Dahlman,J., Cheng,A., Hall,B.M., Qualman,S.J., Chandler,D.S., *et al.* (2008) NF-kappaB-YY1-miR-29 regulatory circuitry in skeletal myogenesis and rhabdomyosarcoma. *Cancer Cell*, **14**, 369–381.
28. Shokri,L., Inukai,S., Hafner,A., Weinand,K., Hens,K., Vedenko,A., Gisselbrecht,S.S., Dainese,R., Bischof,J., Furger,E., *et al.* (2019) A comprehensive Drosophila melanogaster transcription factor interactome. *Cell Rep.*, **27**, 955–970.
29. Li,Y., Li,S., Li,R., Xu,J., Jin,P., Chen,L. and Ma,F. (2017) Genome-wide miRNA screening reveals miR-310 family members negatively regulate the immune response in Drosophila melanogaster via co-targeting drosomycin. *Dev. Comp. Immunol.*, **68**, 34–45.
30. Larkin,A., Marygold,S.J., Antonazzo,G., Attrill,H., Dos Santos,G., Garapati,P.V., Goodman,J.L., Gramates,L.S., Millburn,G., Strelets,V.B., *et al.* (2021) FlyBase: updates to the Drosophila melanogaster knowledge base. *Nucleic Acids Res.*, **49**, D899–D907.
31. Ruby,J.G., Stark,A., Johnston,W.K., Kellis,M., Bartel,D.P. and Lai,E.C. (2007) Evolution, biogenesis, expression, and target predictions of a substantially expanded set of Drosophila microRNAs. *Genome Res.*, **17**, 1850–1864.
32. Enright,A.J., John,B., Gaul,U., Tuschl,T., Sander,C. and Marks,D.S. (2003) MicroRNA targets in drosophila. *Genome Biol.*, **5**, R1.
33. Messeguer,X., Escudero,R., Farre,D., Nunez,O., Martinez,J. and Alba,M.M. (2002) PROMO: detection of known transcription regulatory elements using species-tailored searches. *Bioinformatics*, **18**, 333–334.
34. Bardou,P., Mariette,J., Escudie,F., Djemiel,C. and Klopp,C. (2014) jvenn: an interactive Venn diagram viewer. *BMC Bioinf.*, **15**, 293.
35. Luo,Y., Hitz,B.C., Gabdank,I., Hilton,J.A., Kagda,M.S., Lam,B., Myers,Z., Sud,P., Jou,J., Lin,K., *et al.* (2020) New developments on the Encyclopedia of DNA Elements (ENCODE) data portal. *Nucleic Acids Res.*, **48**, D882–D889.
36. mod,E.C., Roy,S., Ernst,J., Kharchenko,P.V., Kheradpour,P., Negre,N., Eaton,M.L., Landolin,J.M., Bristow,C.A., Ma,L., *et al.* (2010) Identification of functional elements and regulatory circuits by Drosophila modENCODE. *Science*, **330**, 1787–1797.
37. Yu,G., Wang,L.G. and He,Q.Y. (2015) ChIPseeker: an R/bioconductor package for ChIP peak annotation, comparison and visualization. *Bioinformatics*, **31**, 2382–2383.
38. Thorvaldsdottir,H., Robinson,J.T. and Mesirov,J.P. (2013) Integrative Genomics Viewer (IGV): high-performance genomics data visualization and exploration. *Brief Bioinform*, **14**, 178–192.
39. Li,R., Zhou,H., Jia,C., Jin,P. and Ma,F. (2020) Drosophila Myc restores immune homeostasis of imd pathway via activating miR-277 to inhibit imd/Tab2. *PLoS Genet.*, **16**, e1008989.
40. Neyen,C., Bretscher,A.J., Binggeli,O. and Lemaitre,B. (2014) Methods to study drosophila immunity. *Methods*, **68**, 116–128.
41. Wang,Z. (2011) The guideline of the design and validation of MiRNA mimics. *Methods Mol. Biol.*, **676**, 211–223.
42. Lyu,J., Chen,Y., Yang,W., Guo,T., Xu,X., Xi,Y., Yang,X. and Ge,W. (2021) The conserved microRNA miR-210 regulates lipid metabolism and photoreceptor maintenance in the drosophila retina. *Cell Death Differ.*, **28**, 764–779.
43. Livak,K.J. and Schmittgen,T.D. (2001) Analysis of relative gene expression data using real-time quantitative PCR and the 2(-Delta Delta C(T)) method. *Methods*, **25**, 402–408.
44. Tedesco,S., De Majo,F., Kim,J., Trenti,A., Trevisi,L., Fadini,G.P., Bolego,C., Zandstra,P.W., Cignarella,A. and Vitiello,L. (2018) Convenience versus biological significance: are PMA-differentiated THP-1 cells a reliable substitute for blood-derived macrophages when studying in vitro polarization? *Front. Pharmacol.*, **9**, 71.
45. Mistry,P., Laird,M.H., Schwarz,R.S., Greene,S., Dyson,T., Snyder,G.A., Xiao,T.S., Chauhan,J., Fletcher,S., Toshchakov,V.Y., *et al.* (2015) Inhibition of TLR2 signaling by small molecule inhibitors targeting a pocket within the TLR2 TIR domain. *Proc. Natl. Acad. Sci. U.S.A.*, **112**, 5455–5460.
46. Gagliardi,M. and Matarazzo,M.R. (2016) RIP: RNA immunoprecipitation. *Methods Mol. Biol.*, **1480**, 73–86.
47. Zhou,H., Li,S., Pan,W., Wu,S., Ma,F. and Jin,P. (2022) Interaction of lncRNA-CR33942 with dif/dorsal facilitates antimicrobial peptide transcriptions and enhances drosophila toll immune responses. *J. Immunol.*, **208**, 1978–1988.
48. Lemaitre,B., Nicolas,E., Michaut,L., Reichhart,J.M. and Hoffmann,J.A. (1996) The dorsoventral regulatory gene cassette spatzle/toll/cactus controls the potent antifungal response in Drosophila adults. *Cell*, **86**, 973–983.
49. Mrinal,N. and Nagaraju,J. (2010) Dynamic repositioning of dorsal to two different kappaB motifs controls its autoregulation during immune response in Drosophila. *J. Biol. Chem.*, **285**, 24206–24216.
50. Flores-Saaib,R.D., Jia,S. and Courey,A.J. (2001) Activation and repression by the C-terminal domain of Dorsal. *Development*, **128**, 1869–1879.
51. Tong,Z., Cui,Q., Wang,J. and Zhou,Y. (2019) TransmiR v2.0: an updated transcription factor-microRNA regulation database. *Nucleic Acids Res.*, **47**, D253–D258.
52. Davis,C.A., Hitz,B.C., Sloan,C.A., Chan,E.T., Davidson,J.M., Gabdank,I., Hilton,J.A., Jain,K., Baymuradov,U.K., Narayanan,A.K., *et al.* (2018) The Encyclopedia of DNA elements (ENCODE): data portal update. *Nucleic Acids Res.*, **46**, D794–D801.
53. Sticht,C., De La Torre,C., Parveen,A. and Gretz,N. (2018) miRWalk: an online resource for prediction of microRNA binding sites. *PLoS One*, **13**, e0206239.
54. Hu,Y., Flockhart,I., Vinayagam,A., Bergwitz,C., Berger,B., Perrimon,N. and Mohr,S.E. (2011) An integrative approach to ortholog prediction for disease-focused and other functional studies. *BMC Bioinf.*, **12**, 357.
55. Hallman,M., Ramet,M. and Ezekowitz,R.A. (2001) Toll-like receptors as sensors of pathogens. *Pediatr. Res.*, **50**, 315–321.
56. Ozinsky,A., Underhill,D.M., Fontenot,J.D., Hajjar,A.M., Smith,K.D., Wilson,C.B., Schroeder,L. and Aderem,A. (2000) The repertoire for pattern recognition of pathogens by the innate immune system is defined by cooperation between toll-like receptors. *Proc. Natl. Acad. Sci. U.S.A.*, **97**, 13766–13771.
57. Georgakilas,G., Vlachos,I.S., Zagganas,K., Vergoulis,T., Paraskevopoulou,M.D., Kanellos,I., Tsanakas,P., Dellis,D., Fevgas,A., Dalamagas,T., *et al.* (2016) DIANA-miRGen v3.0: accurate characterization of microRNA promoters and their regulators. *Nucleic Acids Res.*, **44**, D190–195.

58. Lu,L.F., Gasteiger,G., Yu,I.S., Chaudhry,A., Hsin,J.P., Lu,Y., Bos,P.D., Lin,L.L., Zawislak,C.L., Cho,S., *et al.* (2015) A single miRNA-mRNA interaction affects the immune response in a context- and cell-type-specific manner. *Immunity*, **43**, 52–64.
59. Mehta,A. and Baltimore,D. (2016) MicroRNAs as regulatory elements in immune system logic. *Nat. Rev. Immunol.*, **16**, 279–294.
60. Huang,X., Le,Q.T. and Giaccia,A.J. (2010) MiR-210–micromanager of the hypoxia pathway. *Trends Mol. Med.*, **16**, 230–237.
61. Niu,Y., Liu,Z., Nian,X., Xu,X. and Zhang,Y. (2019) miR-210 controls the evening phase of circadian locomotor rhythms through repression of Fasciclin 2. *PLoS Genet.*, **15**, e1007655.
62. Cusumano,P., Biscontin,A., Sandrelli,F., Mazzotta,G.M., Tregnago,C., De Pitta,C. and Costa,R. (2018) Modulation of miR-210 alters phasing of circadian locomotor activity and impairs projections of PDF clock neurons in Drosophila melanogaster. *PLoS Genet.*, **14**, e1007500.
63. Hui,X., Al-Ward,H., Shaher,F., Liu,C.Y. and Liu,N. (2019) The role of miR-210 in the biological system: a current overview. *Hum. Hered.*, **84**, 233–239.
64. Bavelloni,A., Ramazzotti,G., Poli,A., Piazzi,M., Focaccia,E., Blalock,W. and Faenza,I. (2017) MiRNA-210: a current overview. *Anticancer Res.*, **37**, 6511–6521.
65. Xie,M., Wang,J., Gong,W., Xu,H., Pan,X., Chen,Y., Ru,S., Wang,H., Chen,X., Zhao,Y., *et al.* (2019) NF-kappaB-driven miR-34a impairs Treg/Th17 balance via targeting Foxp3. *J. Autoimmun.*, **102**, 96–113.
66. Kohanbash,G. and Okada,H. (2012) MicroRNAs and STAT interplay. *Semin. Cancer Biol.*, **22**, 70–75.
67. Huang,X., Ding,L., Bennewith,K.L., Tong,R.T., Welford,S.M., Ang,K.K., Story,M., Le,Q.T. and Giaccia,A.J. (2009) Hypoxia-inducible mir-210 regulates normoxic gene expression involved in tumor initiation. *Mol. Cell*, **35**, 856–867.
68. Ivan,M., Harris,A.L., Martelli,F. and Kulshreshtha,R. (2008) Hypoxia response and microRNAs: no longer two separate worlds. *J. Cell. Mol. Med.*, **12**, 1426–1431.
69. Manfruelli,P., Reichhart,J.M., Steward,R., Hoffmann,J.A. and Lemaitre,B. (1999) A mosaic analysis in Drosophila fat body cells of the control of antimicrobial peptide genes by the Rel proteins Dorsal and DIF. *EMBO J.*, **18**, 3380–3391.
70. Qu,X., Han,J., Zhang,Y., Wang,X., Fan,H., Hua,F. and Yao,R. (2019) TLR4-RelA-miR-30a signal pathway regulates Th17 differentiation during experimental autoimmune encephalomyelitis development. *J. Neuroinflamm.*, **16**, 183.
71. Kurshakova,M., Maksimenko,O., Golovnin,A., Pulina,M., Georgieva,S., Georgiev,P. and Krasnov,A. (2007) Evolutionarily conserved E(y)2/Sus1 protein is essential for the barrier activity of Su(Hw)-dependent insulators in Drosophila. *Mol. Cell*, **27**, 332–338.
72. Wei,W. and Brennan,M.D. (2000) Polarity of transcriptional enhancement revealed by an insulator element. *Proc. Natl. Acad. Sci. U.S.A.*, **97**, 14518–14523.
73. Melnikova,L., Molodina,V., Erokhin,M., Georgiev,P. and Golovnin,A. (2019) HIPP1 stabilizes the interaction between CP190 and Su(Hw) in the Drosophila insulator complex. *Sci. Rep.*, **9**, 19102.
74. Kyrchanova,O., Chetverina,D., Maksimenko,O., Kullyev,A. and Georgiev,P. (2008) Orientation-dependent interaction between Drosophila insulators is a property of this class of regulatory elements. *Nucleic Acids Res.*, **36**, 7019–7028.
75. Kuhn,E.J., Viering,M.M., Rhodes,K.M. and Geyer,P.K. (2003) A test of insulator interactions in Drosophila. *EMBO J.*, **22**, 2463–2471.
76. Golovnin,A., Melnikova,L., Babosha,V., Pokholkova,G.V., Slovohotov,I., Umnova,A., Maksimenko,O., Zhimulev,I.F. and Georgiev,P. (2023) The N-terminal part of Drosophila CP190 is a platform for interaction with multiple architectural proteins. *Int. J. Mol. Sci.*, 24.
77. Kaushal,A., Dorier,J., Wang,B., Mohana,G., Taschner,M., Cousin,P., Waridel,P., Iseli,C., Semenova,A., Restrepo,S., *et al.* (2022) Essential role of Cp190 in physical and regulatory boundary formation. *Sci. Adv.*, **8**, eabl8834.
78. Bag,I., Chen,S., Rosin,L.F., Chen,Y., Liu,C.Y., Yu,G.Y. and Lei,E.P. (2021) M1BP cooperates with CP190 to activate transcription at TAD borders and promote chromatin insulator activity. *Nat. Commun.*, **12**, 4170.
79. Melnikova,L., Kostyuchenko,M., Molodina,V., Parshikov,A., Georgiev,P. and Golovnin,A. (2017) Multiple interactions are involved in a highly specific association of the Mod(mdg4)-67.2 isoform with the Su(Hw) sites in Drosophila. *Open Biol*, 7.
80. Goguet-Rubio,P., Seyran,B., Gayte,L., Bernex,F., Sutter,A., Delpech,H., Linares,L.K., Riscal,R., Repond,C., Rodier,G., *et al.* (2016) E4F1-mediated control of pyruvate dehydrogenase activity is essential for skin homeostasis. *Proc. Natl. Acad. Sci. U.S.A.*, **113**, 11004–11009.
81. Caramel,J., Lacroix,M., Le Cam,L. and Sardet,C. (2011) E4F1 connects the Bmi1-ARF-p53 pathway to epidermal stem cell-dependent skin homeostasis. *Cell Cycle*, **10**, 866–867.
82. Lacroix,M., Caramel,J., Goguet-Rubio,P., Linares,L.K., Estrach,S., Hatchi,E., Rodier,G., Lledo,G., de Bettignies,C., Thepot,A., *et al.* (2010) Transcription factor E4F1 is essential for epidermal stem cell maintenance and skin homeostasis. *Proc. Natl. Acad. Sci. U.S.A.*, **107**, 21076–21081.
83. Hatchi,E., Rodier,G., Sardet,C. and Le Cam,L. (2011) E4F1 dysfunction results in autophagic cell death in myeloid leukemic cells. *Autophagy*, **7**, 1566–1567.
84. Hatchi,E., Rodier,G., Lacroix,M., Caramel,J., Kirsh,O., Jacquet,C., Schrepfer,E., Lagarrigue,S., Linares,L.K., Lledo,G., *et al.* (2011) E4F1 deficiency results in oxidative stress-mediated cell death of leukemic cells. *J. Exp. Med.*, **208**, 1403–1417.
85. Moison,C., Chagraoui,J., Caron,M.C., Gagne,J.P., Coulombe,Y., Poirier,G.G., Masson,J.Y. and Sauvageau,G. (2021) Zinc finger protein E4F1 cooperates with PARP-1 and BRG1 to promote DNA double-strand break repair. *Proc. Natl. Acad. Sci. U.S.A.*, **118**, e201940811.


**Received:** January 17, 2024. **Revised:** April 25, 2024. **Editorial Decision:** April 27, 2024. **Accepted:** April 30, 2024